1963

Solid support characteristics and plate height in gas chromatography

Judson Morse Harper
Iowa State University

SOLID SUPPORT CHARACTERISTICS AND PLATE HEIGHT IN GAS CHROMATOGRAPHY

by

Judson Morse Harper

A Dissertation Submitted to the
Graduate Faculty in Partial Fulfillment of
The Requirements for the Degree of
DOCTOR OF PHILOSOPHY

Major Subject: Food Technology

Approved:

Signature was redacted for privacy.

In Charge of Major Work

Signature was redacted for privacy.

Head of Major Department

Signature was redacted for privacy.

Dean of Graduate College

Iowa State University
of Science and Technology
Ames, Iowa
1963

TABLE OF CONTENTS

	Page
INTRODUCTION	1
LITERATURE REVIEW	4
Historical Development	4
Non-equilibrium Theory of Gas Chromatography	5
Eddy Diffusion	7
Longitudinal Diffusion	8
Non-equilibrium in the Gas Phase	9
Non-equilibrium in the Liquid Phase	10
Solid Support	12
EXPERIMENTAL	14
Chromatographic Supports	14
Gas Chromatograph	20
Column Evaluation	22
THEORY AND CALCULATIONS	24
Calculation of Plate Height	25
Calculation of Gas Velocity	25
Estimation of Constants by Least Squares Regression	26
Calculation of Constants	27
Estimation of Diffusivities	29
Inter- and Intraparticle Void Volume	30
RESULTS AND DISCUSSION	31
Preliminary Investigations	31
Solid Support Characteristics	36

	Page
van Deemter Equation Constants	41
Eddy Diffusion	42a
Longitudinal Diffusion	50
Gas Phase Resistance to Mass Transfer	59
Liquid Phase Resistance to Mass Transfer	64
CONCLUSIONS	67
SUMMARY	72
BIBLIOGRAPHY	74
ACKNOWLEDGEMENTS	80

NOMENCLATURE

A, A_c	eddy diffusion contribution to plate height, cm.
B, B', B_c'	longitudinal diffusion contribution to plate height, $cm.^2$ $sec.^{-1}$
c	construction factor
C	lumped mass transfer resistances, $C_g' + C_l f/p_o$
C_c'	diffusion term in the coupled eddy diffusion contribution, sec.
C_g, C_g'	gas phase resistance to mass transfer contribution to plate height, sec.
C_l	liquid phase resistance to mass transfer contribution to plate height, sec.
CP	Chromosorb P
d	distance to peak maximum, cm.
d_p	particle diameter, cm.
D	diffusivity, $cm.^2$ $sec.^{-1}$
D_g'	diffusivity of solute in gas phase, $cm.^2$ $sec.^{-1}$
f	compressibility factor
F_o	volume flow rate at column temperature and pressure, $cm.^3$ $sec.^{-1}$
H	height of a theoretical plate, cm.
k	capacity ratio, $(t_r - t_a)/t_a$
l	length of column, cm.
L	% w liquid phase on an equal volume of CP
m	mass of sample, g.
m_p	mass of packing, g.
M	mass of pycnometer, g.
n	number of theoretical plates

p_i	column inlet pressure, atm.
p_o	column outlet pressure, atm.
Q	liquid phase per 100 ml. packing, g.
S	cross sectional area of tube, cm.^{2}
t_a	retention time of non-absorbed gas, sec.
t_r	retention time of solute, sec.
T	tortuosity
u	velocity, cm. sec.$^{-1}$
u_a'	velocity in intra- and interparticle space at p_o and column temperature, cm. sec.$^{-1}$
u_o	interparticle velocity at p_o and column temperature, cm. sec.$^{-1}$
u'	interparticle velocity at p_o = 1 atm. and column temperature, cm. sec.$^{-1}$
$\bar{u}$	$u_o f$, average column velocity
V_a	retention volume of air peak, cm.^{3}
V_c	volume of empty column, cm.^{3}
V_d	dead volume of sample heater and cell, cm.^{3}
V_l	liquid phase volume, cm.^{3}
V_p	intraparticle volume, cm.^{3}
V_s	true solid support volume, cm.^{3}
V_v	interparticle volume, cm.^{3}
w	peak width at base, cm.
x	length, cm.
β	coupled eddy diffusion term
γ, γ_v, γ_p	labyrinth constant
ϵ	interparticle void fraction

λ	eddy diffusion coefficient
ρ_b	packed density, g. cm.$^{-3}$
ρ_l	liquid phase density, g. cm.$^{-3}$
ρ_p	particle density, g. cm.$^{-3}$
ρ_s	true support density, g. cm.$^{-3}$
ω_{fi}	contribution to C_g' due to flow inhomogenity
ω_{si}	contribution to C_g' due to solvent inhomogenity

INTRODUCTION

Gas chromatography is playing an increasingly important role in food technology. It has been successfully applied to diverse analytical and quality control problems in food technology such as: 1) flavor identification, 2) fermentation control, 3) fatty acid analysis, 4) pesticide residue detection, 5) glyceride structure analysis and 6) control of flavor uniformity. To further expand gas chromatography's usefulness in these areas and to have it perform yet more definitive tasks, a better understanding of the theory of operation is required.

Chromatography is a physical method of separation employing two phases, one a stationary phase of large surface area and the other a mobile phase, or eluting fluid, which percolates through the stationary phase. In gas chromatography, the stationary phase is a liquid. This liquid is usually coated on the surface of a fine granular porous solid to increase its exposed surface and improve mass transfer between the mobile and stationary phases. This coated solid support is packed into a small diameter column which is placed in a thermostated oven. The mobile phase is a stream of gas, usually helium, hydrogen or nitrogen. When a small quantity of volatilized liquid or gaseous sample is introduced into the gas stream at the beginning of the column, it distributes itself between the two phases. Because an equilibrium condi-

tion controls the distribution of the sample, the ratio of the concentration of the sample in the two phases (partition coefficient) is usually almost constant for a given compound. The portion of the sample in the liquid phase re-enters the gas stream as the concentration there is depleted by the movement of the eluting gas. The process of partitioning between the two phases continues until the compound is swept through the column. The width of the elution band, as the compound proceeds down the column, widens because of non-equilibrium in the diffusion processes in the mobile and stationary phases. Separation occurs when the partition coefficients are different for the sample compounds; the amount of separation is a function of the ratio of partition coefficients. As the compounds emerge from the end of the column, their presence in the gas stream is detected using a thermal conductivity cell or other detection device. An electrical signal proportional to the concentration is sent to a millivolt strip chart recorder which shows each component as a peak on the chart.

The solid support used in preparing the column plays an extremely important role in the performance of the column, because its configuration influences the distribution of the stationary phase and the contact between the mobile and stationary phases. Many materials have been used as solid supports with diatomaceous earth and firebrick finding the greatest acceptance. Studies have been made on the various solid supports which are commercially available to ascertain

their contribution to column efficiency (2, 21, 62) but variation in the chemical composition of these supports has made it difficult to determine the effect of the support structure.

Desty and Harbourn (19) and Decora and Dineen (13) used the commercial detergent Tide as a solid support in gas chromatography. This suggested that a solid support, whose properties could be easily varied, could be prepared by drying various inorganic salts to form a porous matrix. A solid support resembling Tide results from lyophilizing a solution of sodium hexametaphosphate, sodium silicate, and sodium sulfate in about the proportion found in commercial Tide. The porosity of this material can be readily changed by adjusting the proportions of water and salt in the solution before drying.

The objective of this study was to determine the effect of the porosity of the support and various stationary phase levels on the efficiency of the gas chromatographic process.

LITERATURE REVIEW

Historical Development

Martin and Synge (55) introduced partition chromatography in 1941 with a system using liquids as both the mobile and stationary phases. In this pioneering paper, the authors perceived future developments by noting that the mobile phase need not be liquid, and that a gas as the mobile phase would lead to more refined separations of volatile substances than was possible with conventional distillation and extraction techniques. Not until 1952 was the idea of gas chromatography investigated by James and Martin (40) who separated volatile fatty acids on a column of kieselguhr impregnated with silicone oil with nitrogen as the eluting gas.

The concentration of the solute emerging from a partition chromatogram forms a Gaussian distribution whose width increases with increasing elution volume. To explain this Gaussian shaped distribution, Martin and Synge (55) and Glueckauf (36) elaborated the plate theory which considers the chromatographic column as consisting of a large number of equivalent plates analogous to an extraction column. Glueckauf (36) and Klinkenberg and Sjenitzer (49) have shown that distribution of a solute in continuously flowing eluent is of the Gaussian type. Their theory also showed that the number of theoretical plates, n, in the column can be calculated from the elution curve by the equation:

$$n = 16 \left(\frac{d}{w} \right)^2 \qquad (1)$$

where d is the distance (or time) from the point of sample injection to the peak maximum and w is the width of the peak at its base. The height equivalent to a theoretical plate, H, is calculated from the above as:

$$H = \frac{l}{n} \qquad (2)$$

where l is the length of the column.

Non-equilibrium Theory of Gas Chromatography

Even though the plate theory accounts for band broadening it does not correlate the operating parameters of the column with plate height. The non-equilibrium or rate theory which accomplishes this was initiated by van Deemter *et al.* (14). They described the diffusional and finite mass transfer effects within the column by differential material balances in the two phases. The solution of these balance equations results in the van Deemter equation:

$$H = A + \frac{B}{u} + C_l u \qquad (3)$$

where u is the gas velocity, A accounts for band broadening due to unequal velocity channels in the packing, B for longitudinal molecular diffusion in the gas phase and C_l for finite rate of mass transfer in the liquid phase. In the derivation of the van Deemter equation, finite rate of mass transfer in the gas phase was omitted because estimates indicated that its contribution would be negligible compared to that of the liquid phase.

In 1953 Golay (37) introduced the use of capillary columns in which the liquid phase is spread in a film on the capillary wall rather than on a porous packing. He derived the theory for band spreading in capillary columns and found that this required a significant gas phase mass transfer (C_g) contribution and pointed to the inclusion of a similar term in the van Deemter equation. Jones (41) included three terms to account for gas phase effects in his non-equilibrium theory. Giddings (24, 28, 29, 31), Bethea and Adams (4), Bohemen and Purnell (6) and Khan (44) have proposed additions to the van Deemter equation to account for C_g effects.

Experimentally, the addition of the $C_g u$ contribution to the van Deemter equation has been confirmed by Bohemen and Purnell (6), Giddings *et al.* (33), Perrett and Purnell (58), Kieselbach (46, 47), De Ford *et al.* (15) and Dal Nogare and Chiu (11). All these workers found C_g was in the order of magnitude of C_l and contributed particularly at low liquid loads when C_l became small. The velocity, u, used in the van Deemter equation must also be corrected for the compression of the mobile gas phase due to pressure changes across the column. Bohemen and Purnell (5) wrote the modified van Deemter equation corrected for gas compression effects as:

$$H = A + \frac{B'}{u'} + C_g' u' + C_l \bar{u} \qquad (4)$$

where

$$u' = p_o u_o \qquad (5)$$

u' = interparticle velocity at unit column outlet pressure, cm. $sec.^{-1}$

p_o = column outlet pressure in atm.

u_o = interparticle velocity at column outlet pressure, cm. $sec.^{-1}$

and $$\bar{u} = u_o f \qquad (6)$$

$\bar{u}$ = average interparticle column velocity, cm. $sec.^{-1}$

f = compressibility factor of James and Martin (40).

Giddings (30) and Giddings *et al.* (33) suggested an additional pressure correction to $A + \frac{B'}{u'} + C_g'u'$ varying between 1 and 9/8 as p_i/p_o varies between zero and infinity.

Eddy Diffusion

The result of unequal velocity flow paths, arising from the packing arrangement of the support particles, on the band spreading in a chromatographic column is termed eddy diffusion. The existence of an eddy diffusion term in flow through packed beds was confirmed by the derivations of Klinkenberg and Sjenitzer (49) using a statistical approach, Carberry and Bretton (9) and Kramers and Alberda (50) using a mixing stage model and Giddings (26) using a random walk model. The first three derivations lead to an eddy diffusion contribution, A, which did not change with u. They concluded $A = 2\lambda d_p$, where $A > d_p$, the particle diameter. Giddings concluded that a coupled eddy diffusion contribution to plate height, A_c, should vary with velocity such that:

$$A_c = \frac{1}{\frac{1}{2\lambda d_p} + \frac{1}{C_c u}} \qquad (7)$$

where $A_c \rightarrow 0$ as $u \rightarrow 0$ and $A_c \rightarrow 2\lambda d_p$ as $u \rightarrow \infty$. The A_c of Giddings was criticized by Klinkenberg and Sjenitzer (48) on statistical grounds.

The exact nature of the A term, as determined by experimental results, has caused considerable controversy. Using graphical and numerical curve fitting methods, values of A = 0 or less than d_p have been found by many workers (1, 7, 8, 15, 32, 33, 45, 56) while others have apparently found negative A values (7, 33, 52, 60). Some evidence has been presented that indicates that A is velocity dependent (7, 35, 60). Many of the above results were obtained by workers who used incorrect methods to obtain the column interparticle velocity. In recent carefully performed work (6, 58), constant A values were obtained which agreed with theory.

The value of λ has been found by some researchers (5, 14, 16, 49, 61) to increase as d_p decreases while others (1, 6) have found it independent of d_p. The usual graphical and numerical curve fitting techniques have been unable to resolve this question.

Longitudinal Diffusion

The $\frac{2\gamma D_g}{u}$ or $\frac{B}{u}$ term of the van Deemter equation accounts for the effect of longitudinal diffusion on band spreading. D_g is the diffusion constant of the solute in the mobile phase and γ is a constant ($\simeq 1$) which corrects D_g for the

tortuosity of the diffusion path through the packing and for area restrictions. No theory exists whereby γ can be predicted from structural considerations except that Giddings (24) hints that $\gamma = cT^{-2}$ where c is a construction factor and T is the tortuosity; however, both c and T are as empirical as γ.

Bohemen and Purnell (5) found B increased while d_p decreased. Bohemen and Purnell (6), Perrett and Purnell (58), and Kieselbach (46) have data, found by graphical and numerical procedures, respectively, that B is relatively independent of liquid load while De Ford et al. (15) showed increases in B as liquid load decreased. The B terms for porous supports were considerably less than those for solid glass beads (Norem (56)) and this was attributed to gas hold-up inside the particle.

Non-equilibrium in the Gas Phase

The C_g term in the modified van Deemter equation results from non-equilibrium in the gas phase. Jones (41) derived an equation containing three terms to account for contributions due to finite mass transfer, velocity distribution and stagnant layers in the gas phase. Bethea and Adams (4) derived two terms to quantitatively account for gas phase mass transfer in pores and the bulk of the gas. Giddings (24) has extended the generalized non-equilibrium theory in the gas phase by deriving equations accounting for: gas in the particle interior (29), column coiling (25) and the interaction

between unequal flow channels (28).

Perrett and Purnell (58) have modified Golay's (37) gas phase mass transfer term, for capillary columns, to apply to packed columns but found that its magnitude was less than 10% of actual C_g values measured. These authors have concluded however, using their own data and that of others, that $C_g \propto d_p^2 D_g^{-1}$ as theory had predicted.

C_g has been theoretically shown to be a function of liquid load (Giddings (28)). Perrett and Purnell (58) found that C_g changed more rapidly with liquid load than the theory predicts. These authors would write:

$$C_g = (\omega_{fi} + \omega_{si}) \frac{d_p^2}{D_g} \qquad (8)$$

where ω_{fi} is the flow inhomogenity contribution proposed by Giddings and ω_{si} is an additional effect due to solvent inhomogenity. The ω coefficients used are functions of liquid load.

Non-equilibrium in the Liquid Phase

In the original work of van Deemter et al. (14) the whole increase in H with increasing u was attributed to finite liquid phase mass transfer rates. Many other workers have derived, from theoretical considerations, the same or similar terms showing:

$$C_l \propto \frac{k}{(1 + k)^2} \cdot \frac{d_f^2}{D_l} \qquad (9)$$

where k = capacity ratio = $\frac{t_r - t_a}{t_a}$

t_r = retention time of solute, sec.

t_a = retention time of non-absorbed gas, sec.

d_f = liquid film thickness, cm.

D_l = diffusivity of solute in liquid phase, $cm.^2\ sec.^{-1}$

This equation indicates C_l contributes little to strongly retained peaks assuming a uniform film on the support. This relation has been confirmed by Kieselbach (46) and De Ford et al. (15).

Giddings has envisioned that the liquid distribution on the solid support plays an important role in the magnitude of the C_l term. From theoretical considerations he derived C_l terms which consider uniform narrow pores (29), pores with a wide mouth compared to depth (24), uniform pores filled to a variable depth (31), narrow pores of varying depths and tapers (27), and liquid diffusion considering adsorption at the gas liquid and liquid solid interfaces (29). Non-uniform liquid distribution has been demonstrated by Baker et al. (2) who showed the smallest pores are preferentially filled with liquid, and by Bohemen and Purnell (6) and by Dal Nogare and Juvet (12) who found a uniform film would not account for high observed C_l values. The C_l in capillary columns is also higher than accounted for by a uniform film model (17, 64). Keller et al. (42) found that column bleed is almost entirely from the initial part of the column, leading to a non-uniform liquid load along the column.

One of the obvious ways to reduce C_l contributions is to reduce the amount of liquid phase. Low load columns have been used (23, 63) to give excellent separation of mixtures as much as 200° below their boiling point, but this technique is limited to small samples and low loads of stationary phase may introduce adsorption effects.

Solid Support

The structure and surface characteristics of the solid support used in the column plays an important role in the various contributions to H in the modified van Deemter equation. Diatomite filter aid was first used as a solid support by James and Martin (40). Baker et al. (2) have examined the physical properties of both the white and pink diatomaceous supports and found their surface area, pore size distribution, pore volume and packed density varied considerably. Bohemen and Purnell (7) demonstrated that support particles in a narrow mesh range and of small diameter improved H. The effect of surface area, pore volume and packed density of supports on resolution was studied by Dimbat (21). He found packed densities between 0.45 and 0.65 g. $cm.^{-3}$ gave satisfactory results. Ettre (22) established that the surface area of the support does not markedly effect separation if it is above the threshold of 1 $m.^2$ $g.^{-1}$.

Other solid supports have been studied such as crushed unglazed tile (54), the commercial detergent Tide (13, 19),

powdered Teflon (51, 62) and glass beads (3, 52, 62). The adsorption characteristics of firebrick, glass beads and Tide were compared by Bens (3) and Tide was most adsorptive with glass beads showing little adsorption. Ottenstein (57) has given a complete review of support materials with considerable emphasis on methods used to reduce adsorption causing tailing of peaks.

EXPERIMENTAL

Chromatographic Supports

Compounding the solid support

The solid support used was a mixture (dry basis) of 11% w sodium sulfate, 70% Calgon (sodium hexametaphosphate) and 19% w sodium silicate. The dry support was prepared by compounding the above mixture in water solutions having solids contents of 42/100 (g. solids/g. water), 50/100, 62/100 and 75/100 for use in preliminary studies and 40/100, 51/100 and 55/100 for the comprehensive studies. When the salts were dissolved in the above proportions, a lumpy gel resulted which was difficult to handle. To avoid problems, the mixture was prepared in batches containing 600 g. water each, with the appropriate amounts of sodium sulfate and Calgon added. This solution and the required amount of 40° Bé sodium silicate were heated separately to 70° and mixed in a Waring Blender for 1 min. The gel formed by the addition of the silicate was uniform after blending and the mixture had a viscosity similar to heavy corn syrup.

Drying the solid support

The blended solid support solution containing 600 g. water was divided into three 1000 ml., 24/40 ⅋ female round bottom glasks. The contents of each flask were frozen by rotating the flask in a bath of dry ice-acetone. When freezing was complete, evidenced by the solid cracking away from

the sides of the flask, the flasks were attached to a laboratory lyophilizer and dried at 0.03 mm. Hg. The sublimed vapors were condensed in a dry ice-acetone trap. The samples remained solid during the drying process which required about 24 hr.

Grinding the solid support

After drying was complete, the solid support was broken up and removed from the flasks. To insure dryness, it was vacuum oven dried at 120° and 28 in. Hg vacuum for an additional 4 hr. The solid support was next ground with a mortar and pestle and sieved to obtain the -40+60 mesh (U. S. Standard Sieve Series) fraction. The ground support was stored in Mason jars with rubber gasketed lids as the support is hygroscopic.

Chromosorb solid support

Johns-Mansville Chromosorb P, non-acid washed, -40+60 mesh fraction was used. This support will be denoted by CP throughout this paper.

Packed density The packed density (g. solid support/ $cm.^3$ of packed volume), ρ_b, of the bare and coated supports was measured with the device and procedure described by Harper (38) using a 25 ml. rather than a 250 ml. graduated cylinder.

Particle density The particle density (g. solid support/$cm.^3$ of particle volume), ρ_p, was measured using the device in Figure 1. A weighted (approx. 4 g.) sample was

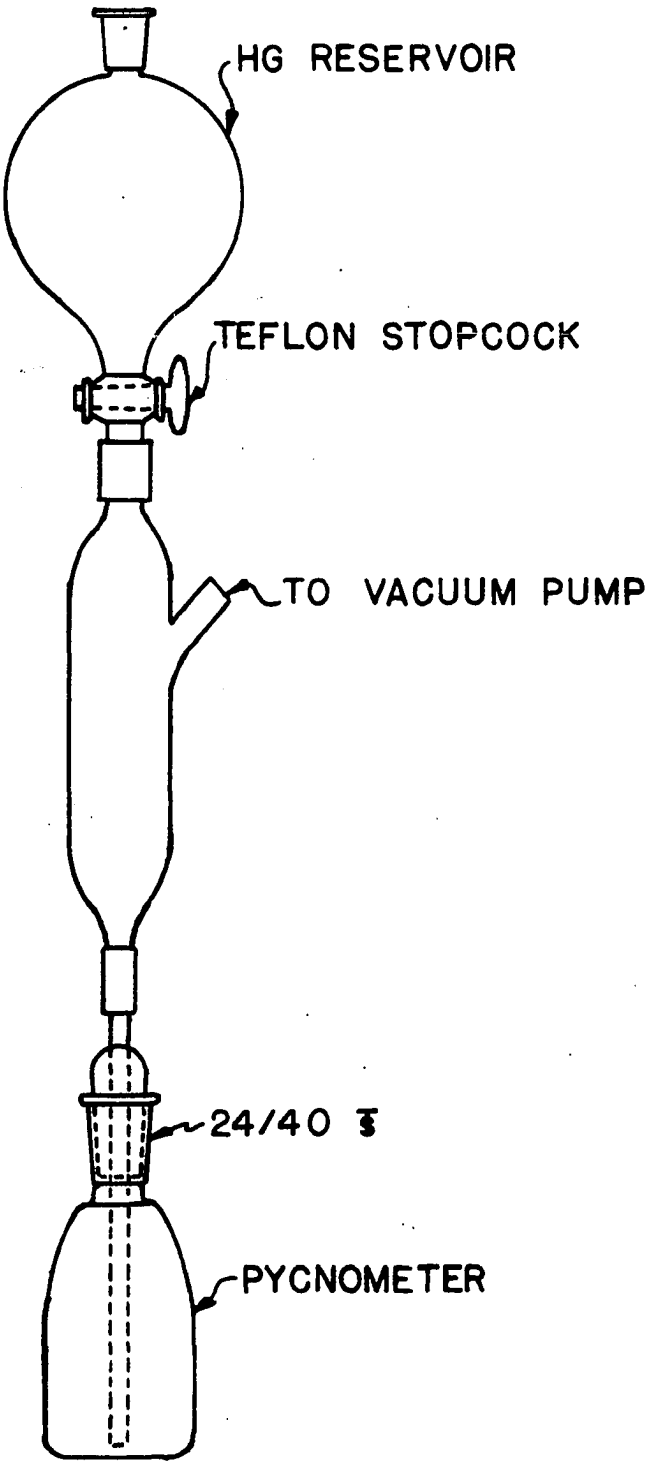

Figure 1. The apparatus used to measure particle density

added to the pycnometer taking care not to fill the tube in its center. All glass-glass and glass-rubber joints were greased and the sample was degassed for 10 min. at less than 0.1 mm. Hg. The stopper on the reservoir was opened after degassing and the mercury allowed to fill the pycnometer; when filling was completed the vacuum was released and the atmospheric pressure applied to the contents of the pycnometer to outline the particles. The filled pycnometer was reweighed and the particle density calculated by the equation:

$$\rho_p = \frac{m \rho_{Hg}}{M_1 + m - M_2} \qquad (10)$$

where ρ_p = particle density

m = mass of sample

M_1 = mass of pycnometer filled with mercury

M_2 = mass of pycnometer and sample when filled with mercury

ρ_{Hg} = density of mercury

The procedure and apparatus described was a simplification of the method described by Cartan and Curtis (10) which required the application of pressure from an outside source to outline the particles.

Pore size distribution for solid support Mercury intrusion pore size distribution data on the dried support was obtained from Prado Laboratories (P. O. Box 2607. Cleveland 7, Ohio). The pores in the range of 100 to 0.035 μ. were measured using an Aminco-Winslow Porosimeter (American Instrument

Co., Inc., Silver Spring, Md.).

Support density The Beckman, Model 930, Air Comparison Pycnometer was used to measure the true support density, ρ_s. Readings of the volume of sample were taken after the sample remained in the pycnometer for 1/2 hr. All determinations using the Air Comparison Pycnometer were made in the laboratories of the U. S. D. A., Agricultural Research Service, Eastern Utilization Research and Development Division, Washington 25, D. C.

Quantity of liquid phase per column

Because the solid supports used had varying packed densities, the amount of liquid phase per volume of column packing was standardized for each liquid load. Most columns in the literature are CP and the amount of liquid, L, is expressed as % w of the CP. The amount of liquid phase per 100 ml. of packing corresponding to a % w liquid load on 100 ml. of CP (ρ_b = 0.412 g. cm.$^{-3}$) is given by:

$$Q = 0.412\ L$$

where Q = g. liquid phase per 100 ml. packing

L = % w liquid phase on CP

Liquid levels of 5 through 30% w, in 5% intervals, were used in this preliminary study and 5 through 25% w, in 10% intervals in the comprehensive studies.

Impregnation of the solid support

100 ml. of solid support was placed in a 500 ml., 24/40 ⅁, female, round bottom flask and heated to 80°. A

quantity of Carbowax 20M equivalent to the liquid load desired was dissolved in 150 ml. acetone by warming. The Carbowax 20M solution was added to the solid support and the acetone removed with a Rinco Rotary Evaporator (Rinco Instrument Co,, Inc., Greenville, Ill.) using a water aspirator for vacuum. After 15 min. evaporation, the coated solid support was placed in a 100° oven for 2 hr. to insure complete removal of acetone. The coated support was resieved to remove any fines resulting from the impregnation procedure.

Packing columns

Six ft. x 0.250 in. o. d. copper refrigeration tubing was used to make the chromatographic columns. The columns were packed with the assistance of an apparatus which held them vertically and vibrated them mechanically using a Dayton 4K-990 Vibrator (Dayton Electric Mfg. Co., Chicago, Ill.) The columns were filled by closing the lower end and slowly pouring the impregnated solid support in the top. The vibration of the columns was continued, accompanied by tapping up and down its length with a hard rubber stick for 30 min. to insure a tight and uniform packing arrangement. The ends of the packed columns were firmly packed with glass wool, after a small amount of coated support was removed, to hold the packing in the column. When not in use, the ends of the columns were stoppered to prevent deterioration by moisture in the air.

Gas Chromatograph

The gas chromatograph used in these studies was assembled in our laboratory and will be described under the headings: chromatographic oven, flow regulation, sample heater, detector and power supply, and recorder.

Chromatographic oven

The oven was divided into two sections, one for the column and the other for the thermal conductivity cell. The column portion of the oven was fitted with an inner cylinder which surrounded the coiled column. Air was circulated with a squirrel cage blower (300 cfm.) up through the inner cylinder and oven walls. Electric heating coils were wound around the outside of the inner cylinder, part of the heaters (600 W.) were controlled with a Variac and the rest (100 W.) with a Wheelco, Model 293C, Capacitrol (Barber-Colman Co., Rockford, Ill.). The temperature in the oven was controlled within $\pm$ 0.1°.

Flow regulation

The pressure of the eluting gas was reduced to approximately 30 psig. with the regulator on the cylinder. The gas first passed through a micro filter and silica gel drying tube (Micro-Tek Instruments, Inc., Baton Rouge, La.). Next a Moore Constant-Differential-Type Flow Controller, Model 63BD-L (Moore Products Co., Philadelphia 24, Pa.) in conjunction with a Hoke 280 Series metering valve (Hoke Incorporated, Cresskill,

N. J.) was used to control and maintain constant flow and compensate for minor down stream pressure fluctuations. The pressure at the inlet of the column was measured with a standardized Bourdon tube pressure gauge. For approximate flow measurement, a Brooks, type 1355, rotameter (Brooks Instrument Co., Inc., Hatfield, Pa.) was located in the gas line before the column.

Sample heater

The sample heater was of a flow through design having a small dead volume (approx. 1 ml.). Heating was accomplished with a 50 W. cartridge heater and the temperature was controlled with a Variac. The syringe used to inject the sample entered the sample heater through a silicone rubber septum which was self-sealing.

Detector and power supply

The presence of sample components in the eluting gas was measured with a Gow-Mac, Model 9285, thermal conductivity cell used in conjunction with a Gow-Mac Power Supply and Bridge Control, Model 9999 (Gow-Mac Instruments Co., Madison, N. J.). The thermal conductivity cell, located below the column section of the oven, was heated separately with six 100 W. cartridge heaters controlled with a Variac. The cell and heaters were surrounded with pea gravel to steady the heat flux and damp out temperature variations.

Recorder

A Brown Electronik recording potentiometer, -0.1 to +1.0 mv. range, (Minneapolis-Honeywell Reg. Co., Brown Instruments Div., Philadelphia, Pa.) continuously recorded the unbalance of the thermal conductivity cell. All chromatograms were made using a chart speed of 30 in./hr.

Column Evaluation

Chromatograph temperatures

All columns were evaluated isothermally using the following chromatograph temperatures: oven, 103 $\pm$ 0.5°; cell, 125 $\pm$ 2°. The columns were conditioned, at a low gas flow, while the instrument temperatures equilibrated over night before evaluation commenced.

Test Compound

The performance of the columns was measured using the test compound 2-octanone (practical) Eastman Organic Chemicals, Distillation Products Industries, Rochester, N. Y.). A 1.0 μl. sample of a 5% solution of 2-octanone in benzene was injected using a Hamilton 10 μl. syringe for each flow rate tested. Reasonable sized peaks (approx. 25% of full scale) resulted from the 1.0 μl. sample. It was also confirmed that plate height was constant for all sample sizes $>$ 2.0 μl.

Eluting gas

In the preliminary study all columns were evaluated with helium. In the comprehensive study, each column was first

evaluated using helium and then nitrogen. A total of 20 to 30 flow rates varying between 0.05 and 6 ml./sec. were used on each column, evaluated in the comprehensive study, with each carrier gas. The bridge circuit was regulated at 250 ma. for helium and 160 ma. for nitrogen. Maximum sensitivity was used for nitrogen and approximately 75% signal attenuation for helium.

Flow rate measurement

The flow at the outlet of the column was measured with a soap bubble meter and stop watch. The inlet pressure to the column was measured using a calibrated Bourdon tube pressure gauge; the outlet pressure with a barometer.

THEORY AND CALCULATIONS

The non-equilibrium theory of chromatography was developed on the assumption that the processes which contribute to band spreading act independently, such that their separate contributions can be added to obtain H, the height equivalent to a theoretical plate. The modified van Deemter equation proposed by Bohemen and Purnell (5),

$$H = A + \frac{B'}{u'} + C_g'u' + C_l \frac{fu'}{p_o}, \qquad (12)$$

is of this form and gives good reproduction of experimental data (6, 58) over a wide range of velocity. It was, therefore, chosen as the basis of treating the data in this work.

The constants in the above equation can be evaluated in several ways. A least squares regression of the experimental data is one approach but was found to be unsatisfactory in this study because many of the evaluated constants were not statistically different from zero. Purnell and co-workers have devised methods using experimental data obtained with two different eluting gases to calculate the constants. Although these methods are long and laborious, constants which gave satisfactory reproduction of experimental data were obtained. These methods will be outlined below. In order to give a better fit of eq. (12) to the experimental data, a new procedure for calculating a coupled eddy diffusion contribution to plate height was developed in this study and it will be described.

Calculation of Plate Height

The elution peaks appearing on a chromatogram result from a Gaussian distribution of the solute in the eluting gas. From these peaks the number of theoretical plates, n, can be calculated using the equation of Glueckauf (36),

$$n = 16 \left(\frac{d}{w} \right)^2, \tag{13}$$

where n = number of theoretical plates

d = distance from point of sample injection to peak maximum

w = width of peak at its base

H is calculated by:

$$H = \frac{l}{n} \tag{14}$$

where l is the length of column.

Calculation of Gas Velocity

Bohemen and Purnell (5) have shown that nearly all the carrier gas flow in the column occurs in the interparticle void. Therefore, the appropriate velocity to be used in the modified van Deemter equation is given by:

$$u_o = \frac{F_o}{\epsilon S} \tag{15}$$

where u_o = outlet interparticle gas velocity, $cm.^3\ sec.^{-1}$

F_o = volume flow rate at column temperature and outlet pressure, p_o, $cm.^3\ sec.^{-1}$

S = cross-sectional area of tube, $cm.^2$

$\epsilon = \frac{V_c - m_p/\rho_p}{V_c}$, interparticle void fraction

m_p = mass of packing, g.

ρ_p = particle density, g. $cm.^{-3}$

V_c = volume of empty column, $cm.^3$

Because the primed terms in the modified van Deemter equation are the values at unit outlet pressure, u_o is adjusted to the velocity, u', at p_o = 1 atm. by the relation $u' = u_o p_o$.

The average interparticle column velocity is calculated using:

$$\bar{u} = u_o f = \frac{u'f}{p_o} \qquad (16)$$

where $\bar{u}$ = average column velocity, cm. $sec.^{-1}$

u_o = outlet interparticle velocity, cm. $sec.^{-1}$

$f = \frac{3}{2}\left[\frac{(p_i/p_o)^2-1}{(p_i/p_o)^3-1}\right]$, compressibility factor (40)

p_i = column inlet pressure, atm.

p_o = column outlet pressure, atm.

Estimation of Constants by Least Squares Regression

The constants, which contribute to plate height, in the eq. 12 can be determined using a least squares regression. The IBM 7074 computor at the Iowa State University Computation Center was used to evaluate the constants from the preliminary data using the 42/100, 50/100, 62/100 and 75/100 solid supports with 10 through 30% liquid load in 5% intervals. The data for each solid support were pooled regardless of liquid load to increase the degrees of freedom. The constants were evaluated using several sets of restrictions. The most

satisfactory set of restrictions was: $A = C_1$, $B' = C_2 + C_3L + C_4L^2$, $C_g' = C_5 + C_6L$ and $C_1 = C_7L$ where $C_1 \ldots 7$ are regression coefficients and L = 10, 15, 20, 25, or 30, the % liquid phase on the support. These restrictions were made on the basis of previously noted trends in the coefficients obtained by other workers (46, 58) and from this work. To conform with theory, the restriction was made that $C_1 = 0$ at $L = 0$.

Calculation of Constants

The modified van Deemter eq. 12 shows that the contribution of C_g' and C_1 to H is quite small at low u' so the equation reduces to:

$$H = A + \frac{B'}{u'} \tag{17}$$

as $u' \rightarrow 0$. Plotting H against large $1/u'$ values gives a straight line and A and B' can be obtained from the intercept and slope, respectively.

Bohemen and Purnell (6) have developed a method of calculating C_g' and C_1 from H vs. u' plots obtained with two different eluting gases. The difference in plate height using different gases and velocities is given by:

$$H_1 - H_2 = (A_1 - A_2) + \left(\frac{B'_1}{u'_1} - \frac{B'_2}{u'_2}\right) + (C_{g'_1}u'_1 - C_{g'_2}u'_2) + (C_{1_1}\bar{u}_1 - C_{1_2}\bar{u}_2) \tag{18}$$

where the subscripts 1 and 2 represent the different gases. In theory both A and C_1 are independent of the gas so that when $\bar{u}_1 = \bar{u}_2$, eq. 18 can be written eliminating A and C_1:

$$\Delta H = H_1 - H_2 = \frac{B'_1}{u'_1} - \frac{B'_2}{u'_2} + C_g'_1 u'_1 - C_g'_2 u'_2. \qquad (19)$$

From theory (6) $B' \propto D_g'$ and $C_g' \propto D_g'^{-1}$, therefore, $B'_1/B'_2 = C_g'_2/C_g'_1 = D_g'_1/D_g'_2$. Using this relationship, C_g' can be calculated with eq. 19 when ΔH at $\bar{u}_1 = \bar{u}_2$ is obtained from a H *vs.* $\bar{u}$ plot and B' is known from eq. 17. The value of C_g' calculated in this manner can be made nearly independent of B' by measuring ΔH at high values of $\bar{u}$ so that B'/u' is small.

Eq. 18 can also be used to evaluate C_1 as described by Perrett and Purnell (59). If u' values are chosen so the ratio $u'_1/u'_2 = D_g'_1/D_g'_2$ (or B'_1/B'_2), the A, B' and C_g' terms will be equal, and

$$\Delta H = H_1 - H_2 = C_1 (\bar{u}_1 - \bar{u}_2). \qquad (20)$$

Values of C_1, independent of A, B' and C_g' if D_g' is known, are most reliable when ΔH and $\Delta\bar{u}$ are large at high u'.

An alternative method of evaluating C_g' and C_1 has been proposed by Bohemen and Purnell (6), but it involves the use of A and B' terms evaluated from eq. 17. Eq. 12 can be written as:

$$\frac{H - A - \frac{B'}{u'}}{u'} = C_g' + \frac{C_1 f}{p_o} = C. \qquad (21)$$

A plot of C against f/p_o should give a straight line with slope of C_1 and intercept of C_g'. If values of H are evaluated at $p_o \simeq 1$ atm., the ratio f/p_o varies between approximately 0.5 and 1.0 and means C_g' results from a rather lengthy extrapolation of the curve casting considerable doubt

on its value. Estimates of C_g' by this method can be improved if data at $f/p_o < 0.5$ and > 1.0 are known. These data can be obtained by evaluating a column at $p_o > 1$ atm. and $p_o < 1$ atm., respectively.

Data from this work at $p_o = 1$ atm. gave values of C which became small at $f/p_o \simeq 1$ and gave a curve with a pronounced downward hook rather than a straight line. Similar tendencies were apparent in the plots of De Ford *et al.* (15) at a fixed p_o when they used this technique to evaluate C_g' and C_l. The constant eddy diffusion term, A, of the van Deemter equation plays a major role in the evaluation of C at low u'. Variation in the eddy diffusion contribution to plate height (A_c) with u' could account for the hook in the plot of eq. 21. A coupled A_c term has been proposed by Giddings (26) such that $A_c \rightarrow 0$ as $u' \rightarrow 0$ and $A_c \rightarrow 2\lambda d_p$ as $u' \rightarrow \infty$. Values of A_c at varying u' can be calculated using eq. 21 and the independently evaluated C_g' and C_l terms as:

$$A_c = H - \frac{B_c'}{u'} - Cu'. \qquad (22)$$

It should be noted that Giddings' theory predicts that the plot H *vs.* $1/u'$ should not be linear but curved upward. B' then becomes B_c', the slope of the asymptote, passing through the origin, to the H *vs.* $1/u'$ curve.

Estimation of Diffusivities

The Gilliland equation (34) was used to estimate D_g'. The molar volume of the 2-octanone was estimated by adding

the atomic volumes of the molecular species in the compound.

Inter- and Intraparticle Void Volume

The empty column volume can be considered as a sum of the interparticle, intraparticle, solid support and liquid phase volumes, i.e.:

$$V_c = V_v + V_p + V_s + V_l \tag{23}$$

where V_c = volume of empty column, $cm.^3$

V_v = interparticle void volume, $cm.^3$

$= \epsilon V_c$

V_p = intraparticle void volume, $cm.^3$

$= (1 - \epsilon)(V_c)(1 - \frac{\rho_p}{\rho_s}) - \frac{m_l}{\rho_l}$

V_s = true solid support volume, $cm.^3$

$= (1 - \epsilon)(V_c)(\frac{\rho_p}{\rho_s})$

V_l = liquid phase volume, $cm.^3$

$= \frac{m_l}{\rho_l}$

The retention volume of a nonabsorbed air sample, V_a, is $V_v + V_p$ and given by:

$$V_a = (F_o)\ (t_a)\ f - V_d \tag{24}$$

where V_a = retention volume of air sample, $cm.^3$

F_o = gas flow rate at column temperature and outlet pressure, $cm.^3\ sec.^{-1}$

t_a = retention time of air peak, sec.

f = compressibility factor

V_d = dead volume of sample heater and cell, $cm.^3$

RESULTS AND DISCUSSION

Preliminary Investigations

Preliminary experiments were made to determine the effect of different support packed densities and liquid loads on H at varying gas velocities. Four lyophilized supports, with widely differing packed densities, were used at liquid loads varying between 10 and 30% in 5% intervals. All columns were evaluated using helium as the eluting gas. To better understand the causes for the experimental differences found in the H vs. u' data, the constants in the modified van Deemter equation were evaluated using a least squares regression of the data. This attempt was unsuccessful, however, because many of the evaluated constants were not statistically significant.

The effect of solid support packed density and liquid load on the H vs. u' curve is shown in Figure 2. The 42/100, 50/100, 62/100, and 75/100 (g. solids/g. water) packings used to obtain these data had packed densities of 0.34, 0.41, 0.67 and 0.77 g. $cm.^{-3}$, respectively, before the stationary phase was applied. The minimum H for the packings decreased as the support packed density decreased to that of the 50/100 support. However, when the least dense 42/100 support was used, slight increases in H, compared to the 50/100 support, were measured. These data were in general agreement with Dimbat (21) who found that supports having a packed density

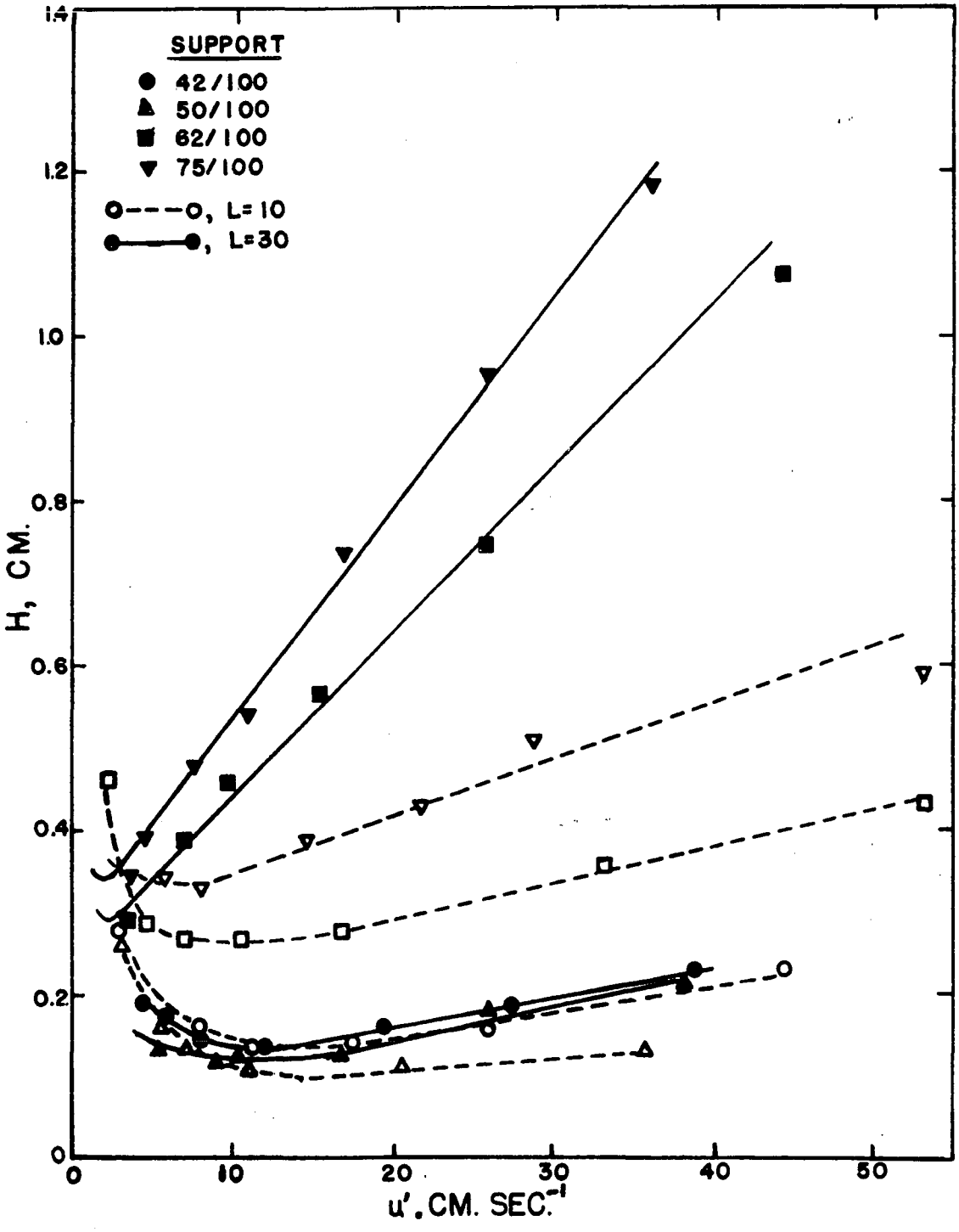

Figure 2. Plate height and interparticle velocity for lyophilized supports of differing packed density at 10 and 30% liquid loads

between 0.45 and 0.65 g. cm.$^{-3}$ gave satisfactory results in gas chromatography.

Increasing the liquid load, L, on the chromatographic supports resulted in marked increases in H at the higher gas velocities. These observations were in agreement with the work in the literature (1, 15, 46, 58) showing the effect of liquid load on H. Figure 2 shows the data for L = 10 and 30, the extremes of the five liquid loads studied on each of the four supports. The increase in H with liquid load was the most pronounced on the packings with the greatest packed density. The least dense 42/100 packing was exceptional in that H did not change appreciably with liquid load at high velocity. The 42/100 packing at low liquid loads was quite fragile and there was some break-up of the support during the column packing procedure. The existence of fines would disturb the flow paths within the column and may cause the exception noted.

The constants in the modified van Deemter equation (eq. 12), which describe the data given in Figure 2, were evaluated using a least squares regression of the pooled data for each support and the results are given in Table 1. Even though good correlation between the data and regression curves was obtained (evidenced by the coefficient of multiple correlation, $R^2 \simeq 1$), many of the constants were not significant at $P < 0.05$. This was particularly true of the C_g' and C_1 constants. This inability to obtain significance in the C_g' and

C_1 constants resulted from the relatively small differences in u' and $\bar{u}$ data used for these regressions making the contributions of these terms difficult to evaluate statistically.

The statistically evaluated constants in Table 1 show A increasing rapidly with support packed density. This finding was not confirmed by the results of the comprehensive studies made in this work. The particularly large value of A for the 75/100 support has doubtful meaning because it was approximately 1.5 times the H minimum measured for this packing. To conform with theory, A must be < H minimum.

These preliminary data indicate that B' decreases with increasing packed density as evidenced in Figure 2 which shows a reduction in u', corresponding to H minimum, with increased packed density. The values of B' obtained using the statistical constants in Table 1 (although many were not significant) show a similar trend with support packed density. The effect of liquid load on B' could not be ascertained because of the general lack of significance in C_3 and C_4, the constants which effect B' as L changes.

The experimental anomaly noted in the statistically evaluated A and the general lack of significance in the regression coefficients for B', C_g' and C_1 point to the weakness of the statistical evaluation of the constants in the modified van Deemter equation. Part of this difficulty resulted from the relatively small numbers of determinations made in the preliminary investigation and the uncertainty in the way which L

Table 1. Values of the van Deemter equation coefficients obtained by least squares regression of the preliminary data[a]

Solid support	d.f.[d]	$A=C_1$, cm.	$B'=C_2+C_3L^b+C_4L^2$, $cm.^2 sec.^{-1}$			$C_g'=C_5+C_6L$, sec.		$C_1=C_7L$, sec.	R^2[c]	Residual mean squares
		$C_1 \times 10^2$	$C_2 \times 10$	$C_3 \times 10^2$	$C_4 \times 10^4$	$C_5 \times 10^3$	$C_6 \times 10^4$	$C_7 \times 10^4$		$s^2 \times 10^3$
42/100	29	2.85* (0.834)[e]	9.14* (1.09)	-2.05 (1.12)	3.18 (2.80)	4.44* (0.373)	-2.65* (0.480)	3.60* (0.610)	0.966	0.0902
50/100	23	3.97* (0.927)	6.21* (0.681)	0.170 (0.799)	-3.05 (2.11)	1.24* (0.489)	0.120 (0.960)	1.16 (1.10)	0.978	0.0391
62/100	26	9.85* (3.60)	16.7* (3.10)	-10.2* (3.49)	19.5* (8.80)	-0.432 (1.31)	-0.814 (2.81)	11.3* (3.65)	0.978	1.07
75/100	24	40.7* (9.51)	-14.6 (7.39)	13.8 (8.22)	-37.3 (20.6)	-5.01 (3.22)	11.6 (8.19)	-3.02 (10.5)	0.954	2.99

[a] The data for each solid support at various liquid loads were pooled.

[b] The % w liquid phase on an equal volume of CP.

[c] Coefficient of multiple correlation.

[d] Degrees of freedem.

[e] Standard error of the measurement.

* Significant ($P < 0.05$).

effects these constants. However, the similarity of u' and $\bar{u}$ will always make it difficult to evaluate C_g' and C_l statistically. To circumvent these problems in the comprehensive study, the constants in the modified van Deemter equation were evaluated using the calculation techniques proposed by Purnell and co-workers.

Solid Support Characteristics

The results of the preliminary studies show that changes in the physical properties of the solid support play an important role in the efficiency of gas chromatography. To better understand how these changes effect plate height, a comprehensive study of four solid supports was made. A summary of the characteristics of the 40/100, 51/100, 55/100 and CP supports used in the comprehensive studies is given in Table 2 and their pore size distributions measured by mercury intrusion in Figures 3a and 3b.

The particle density of the lyophilized supports was fixed by the concentration of salts in the lyophilized mixture; the lower the concentration, the lower the density. This indicates that the cross-linked gel structure which formed when the salts were mixed, was more open when greater amounts of water were present. The particle density increased $\simeq 0.08$ g.cm.$^{-3}$ with each 10% increase in liquid phase regardless of the support. This was an expected result since the amount of liquid phase per packed volume had been standardized

Table 2. Summary of the characteristics of the solid supports used in the comprehensive studies

Solid support	Liquid load, L[a]	Particle density, ρ_p[b]	Packed density, ρ_b[b]	Support density ρ_s[b]	Intra-particle void fraction	Mean pore dia., μ.
40/100	0	0.630	0.301	2.74	0.77	2.4
	5	0.657	0.330			
	15	0.737	0.360			
	25	0.817	0.372			
51/100	0	0.942	0.454	2.78	0.66	1.8
	5	0.981	0.490			
	15	1.04	0.525			
	25	1.12	0.538			
55/100	0	1.16	0.573	2.75	0.58	0.96
	5	1.19	0.604			
	15	1.26	0.640			
	25	1.36	0.687			
CP	0	0.759	0.380	2.47	0.69	0.95[c]
	5	0.788	0.410			
	15	0.870	0.451			
	25	0.953	0.498			

[a]The % w liquid phase on an equal volume of CP.

[b]All densities in g. cm.$^{-3}$

[c]Data of Baker *et al.* (2).

Figure 3a. Pore size distribution of supports
Pores -100+70μ. denoted by $\frac{100}{70}$, volume
fraction of pores < 20μ (intraparticle pores)
add to 1.0

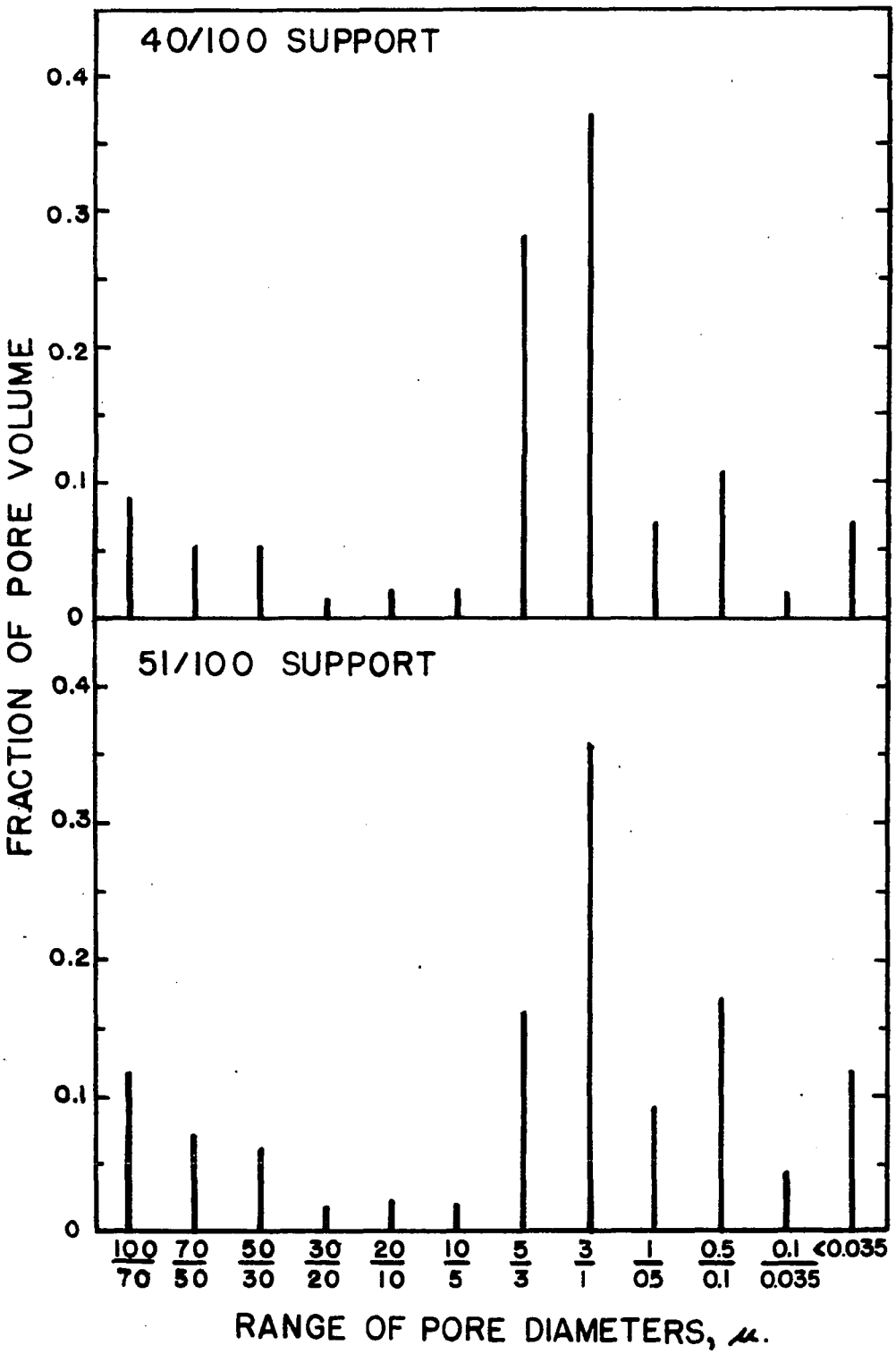
40/100 SUPPORT
51/100 SUPPORT
FRACTION OF PORE VOLUME
0.4
0.3
0.2
0.1
0
100/70
70/50
50/30
30/20
20/10
10/5
5/3
3/1
1/05
0.5/0.1
0.1/0.035
<0.035
RANGE OF PORE DIAMETERS, μ.

Figure 3b. Pore size distribution of supports
Pores -100+70μ. denoted by $\frac{100}{70}$, volume fraction of pores $< 20\mu$ (intraparticle pores) add to 1.0

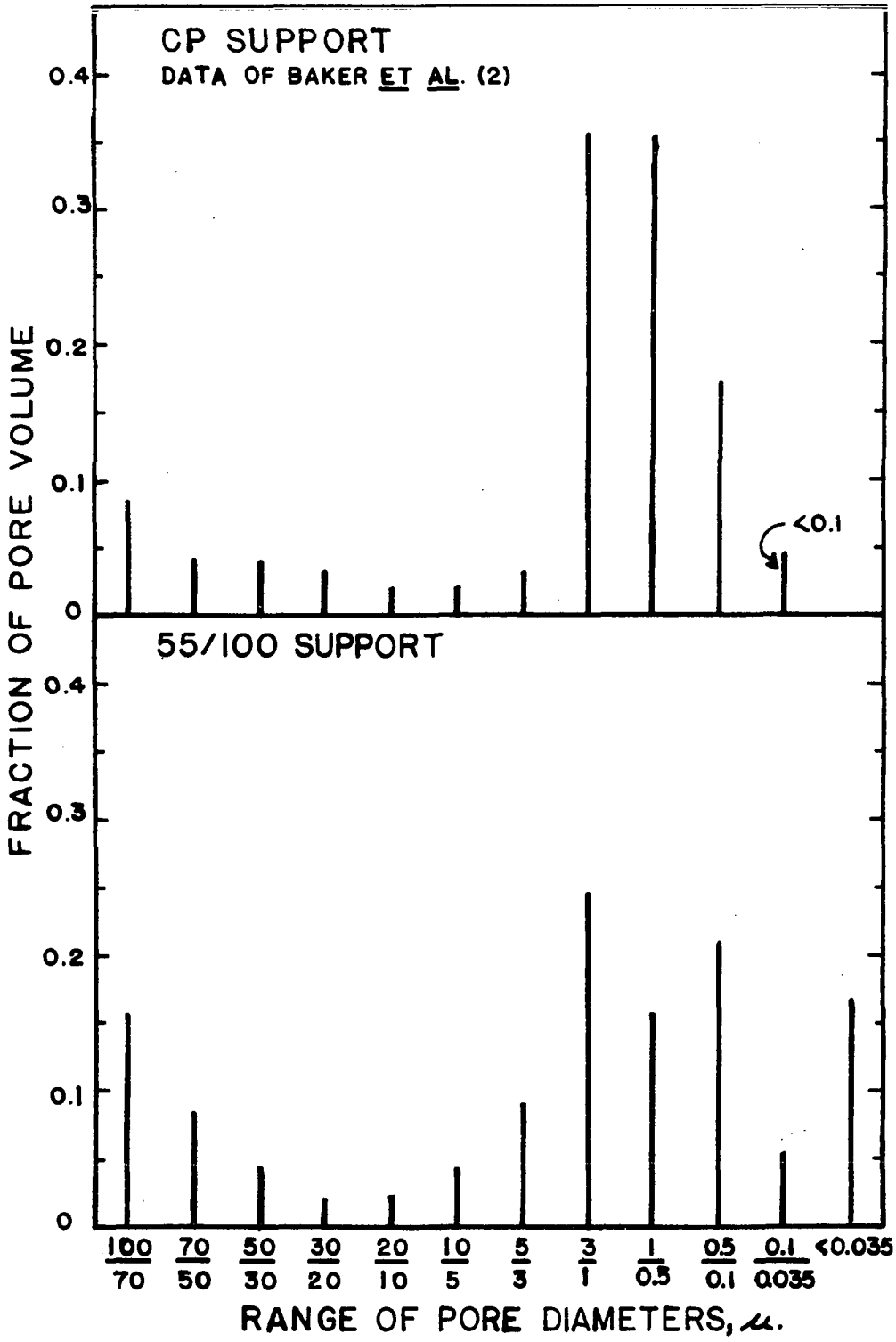
CP SUPPORT
DATA OF BAKER ET AL. (2)
55/100 SUPPORT
FRACTION OF PORE VOLUME
0.4
0.3
0.2
0.1
0
<0.1
100/70
70/50
50/30
30/20
20/10
10/5
5/3
3/1
1/0.5
0.5/0.1
0.1/0.035
<0.035
RANGE OF PORE DIAMETERS, μ.

for each liquid load.

In order for the packed density to be a true measure of change in support characteristics, a packing procedure which produces similar particle arrangements must be used. The data in Table 2 indicate that the packed density was approximately half the particle density for all supports and liquid loads. This result would indicate that the packed density apparatus used for this determination produced similar packing arrangements which contained approximately 50% interparticle void. The packed density can be used as an approximate screening technique to measure changes in the intraparticle void volume of bare and impregnated supports.

The measurement of the particle density requires that the particles must be outlined but not penetrated by the mercury used to fill the pycnometer. Calculations showed that the mercury would penetrate spaces having a 15 μ. diameter when subjected to 1 atm. pressure. The mercury intrusion pore size distribution data was interpreted* assuming that all pores $< 20\ \mu$. were intraparticle spaces. This choice was indicated by the point of minimum intrusion on the pore size distributions at 20 μ. (see Figures 3a and 3b). The pore size distribution data indicate that the 1 atm. pressure applied to the mercury in the pycnometer was sufficient to

---

*Winslow, N. M., Prado Laboratories, Cleveland, Ohio. Data from the pore size distribution. Private communication. 1963.

give accurate results.

The pore size distribution (see Figures 3a and 3b) of the more porous 40/100 support was skewed to the larger 5/3 μ. sizes while the 55/100 support had a more uniform distribution in the range of 3/0.1 μ. The pores $< 0.035\,\mu$. contributed to an increasing extent as the support particle density increased.

The CP support was different from the lyophilized supports because its pore size distribution was nearly all in the 3/0.1 μ. with little $< 0.1\,\mu$. This might be expected when viewing the photographs of the fused diatomite CP support (Ottenstein (57)) which show uniform symetrically arranged diatom valves of approximately 1 - 2 μ. dia. The pores of the lyophilized support were visualized as a randomly dispersed interconnected labyrinth with large numbers of fine pores.

The lyophilized supports gave symetrical elution peaks, but had a tendency to tail at low liquid loads. The CP support used showed less tailing tendency, indicating fewer adsorption sites on its surface.

van Deemter Equation Constants

The effects of changes in solid support characteristics and liquid load on the coefficients contributing to plate height in the modified van Deemter equation are summarized in Table 3. These constants were calculated using the methods of Purnell and co-workers (see Theory and Calculations) where the eddy diffusion coefficients were assumed

constant with changes in velocity.

Figure 4 gives a typical illustration of the fit of experimental data with the curve calculated from the coefficients in Table 3 for 51/100 support at L = 15. The fit is reasonably good with noticable discrepancy at the minimum H. In the following sections this discrepancy will be discussed along with the effect of the chromatographic support and liquid load on the constants of the modified van Deemter equation.

Eddy Diffusion

The exact nature of the eddy diffusion term, resulting from unequal velocity channels in the packing, has been the topic of speculation and controversy in the literature. The results in Table 3, measured from the intercept of the H vs. 1/u' plot, indicate that an eddy diffusion term ($A = 2\lambda d_p$) exists and has a magnitude $> d_p$ ($d_p = 297\mu$). These data show that A for chromosorb was smaller than the values for the lyophilized support. This must result from more unequal velocity channels and/or fewer lateral connections in the columns of lyophilized support. Increases in liquid load and particle density were associated with increases in A for all supports except the 40/100 support. This trend was less apparent in the results found using the coupled eddy diffusion theory (see discussion below and Table 4) and was attributed to general errors in evaluating the A terms. The

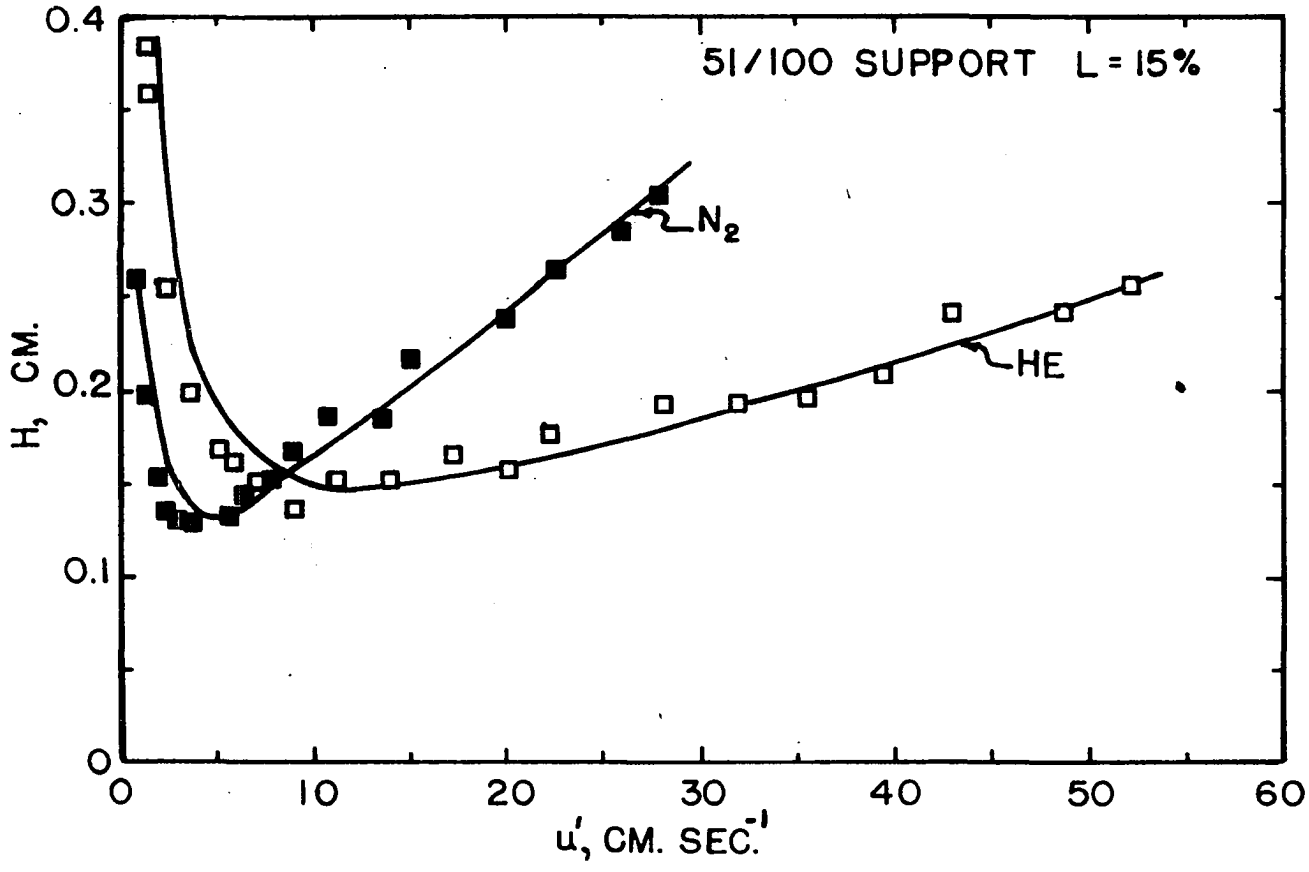

Figure 4. Illustration of fit of experimental data to curve calculated with modified van Deemter equation coefficients from Table 3

Table 3. Calculated van Deemter equation coefficients

Solid support	Liquid load, L[b]	A, cm.	B'_1,[a] $cm.^2 sec.^{-1}$	B'_2, $cm.^2 sec.^{-1}$	$C_g'_1 \times 10^3$, sec.	$C_g'_2 \times 10^3$, sec.	$C_1 \times 10^3$, sec.
40/100	25	0.075	0.56	0.19	1.3	3.8	3.9
	15	0.090	0.67	0.24	2.5	7.4	2.1
	5	0.080	0.84	0.28	3.6	11.	0.90
51/100	25	0.055	0.54	0.17	3.2	9.5	2.8
	15	0.050	0.60	0.20	2.3	7.0	2.0
	5	0.040	0.68	0.22	1.5	4.6	0.91
55/100	25	0.080	0.31	0.10	4.0	12.	9.5
	15	0.065	0.41	0.15	2.5	7.4	2.2
	5	0.055	0.56	0.18	1.8	5.3	1.6
CP	25	0.045	0.62	0.22	4.2	12.	2.1
	15	0.040	0.66	0.24	2.8	8.2	1.3
	5	0.045	0.72	0.26	1.2	3.5	0.81

[a]Subscripts 1 and 2 represent helium and nitrogen, respectively.

[b]The % w liquid phase on an equal volume of CP.

fragility of the 40/100 support at low liquid loads resulted in some particle break-up and the resulting wide particle size might be expected to increase A.

Values of λ lie between 0.65 and 1.5 with $\overline{\lambda} = 1.0$. These are in agreement with similar data reported in the literature (5, 6) and the theoretical meaning of λ (9, 49, 50).

The inability for the curve, calculated with the van Deemter equation using the coefficients in Table 3, to fit the experimental data (see Figure 4) at low velocities and the pronounced hook in the C vs. f/p_o plot (described p. 29) pointed to an A value which varies with velocity. Giddings' coupled eddy diffusion term, A_c, varies with velocity as predicted by the random walk model:

$$H = \frac{1}{\frac{1}{2\lambda d_p} + \frac{1}{C_c' u'}} + \frac{B_c'}{u'} + Cu' = A_c + \frac{B_c'}{u'} + Cu' \qquad (25)$$

where the subscript c denotes terms associated with the coupled theory. Using the independently derived values of B_c', C_g' and C_l, in conjunction with a C vs. f/p_o plot, values of A_c at varying u' were found. Typical plots of A_c vs. u' are given in Figure 5. The slope of Figure 5 equals C_c' as $u' \rightarrow 0$ and $2\lambda d_p$ can be estimated from A_c maximum. These plots are similar to the plots given by Glueckauf (35) who observed the spread of a point source of radioactive HI washed through glass beads with acidified water. A summary of the coefficients for the coupled eddy diffusion term are given in Table 4.

Table 4. Summary of the coefficients for the coupled eddy diffusion term

Solid support	Liquid load, L[d]	$B_{c}'1$[a] $cm.^2 sec.^{-1}$	$B_{c}'2$ $cm.^2 sec.^{-1}$	$C_{c}'1 \times 10^3$, sec.	$C_{c}'2 \times 10^3$ sec.	$C_{c}'2/C_{c}'1$ (theor.=3.0)	A,[b] cm.	$2\lambda_1 d_p$,[c] cm.	$2\lambda_2 d_p$, cm.
40/100	25	0.62	0.23	4.8	13.2	2.76	0.075	0.079	0.064
	15	0.75	0.26	5.9	13.8	2.35	0.090	0.090	0.077
	5	0.90	0.30	16.2	11.6	0.72	0.080	0.075	0.083
51/100	25	0.57	0.20	7.1	12.0	1.69	0.055	0.070	0.065
	15	0.65	0.22	3.9	5.7	1.46	0.050	0.060	0.057
	5	0.71	0.24	5.4	11.0	2.04	0.040	0.038	0.038
55/100	25	0.36	0.12	10.0	23.0	2.30	0.080	0.069	0.073
	15	0.47	0.16	10.5	14.5	1.38	0.065	0.069	0.068
	5	0.60	0.20	12.8	12.8	1.00	0.055	0.062	0.062
CP	25	0.65	0.23	3.0	6.9	2.30	0.045	0.046	0.046
	15	0.69	0.25	1.8	4.4	2.42	0.040	0.039	0.040
	5	0.74	0.27	2.9	7.1	2.42	0.045	0.042	0.040

[a]Subscripts 1 and 2 represent helium and nitrogen, respectively.

[b]Intercept of the H vs. 1/u' plot.

[c]A_c maximum as $u' \longrightarrow 0$.

[d]The % w liquid phase on an equal volume of CP.

The existence of the A_c term is clearly shown by the typical data in Figure 5. Giddings (26) predicted from theoretical considerations that $C_c' = \frac{(\beta d_p)^2}{2 D_g'}$, where βd_p is the distance of a complete diffusion step in the random walk model with β in the order of unity. Values for $C_c'_1 = 0.0018$ and $C_c'_2 = 0.0054$ sec. were calculated using $\beta = 1$, $d_p = 297$ μ. and $D_g'_1 = 0.255$ and $D_g'_2 = 0.0834$ cm.^{2} sec.$^{-1}$ These values are in good agreement with data for CP considering the error in measuring C_c'. Because C_c' was larger for the lyophilized supports, β ranged between 1.5 and 3.0 with some evidence that β increases with λ. This means that the distance a molecule must diffuse to complete a step in the random walk model is proportional to the distance a velocity path persists. C_c' values are somewhat larger than the corresponding C_g' values but they both seem to be influenced in a similar manner by liquid load and particle density. This will be discussed further in the sections on Longitudinal Diffusion and Gas Phase Resistance to Mass Transfer.

The dependence of C_c' on D_g' can be confirmed using the relationship $C_c'_2/C_c'_1 = D_g'_1/D_g'_2$. The ratio $(C_c'_2/C_c'_1)$ of experimentally determined values of C_c' is given in Table 4 and should $\simeq 3.0$, the ratio of the diffusivities found using the Gilliland equation. It should be noted that all experimental ratios are < 3 with more than half > 2 and only one < 1. Due to fluctuations in the experimental data, which strongly influence A_c determined by a difference, and the uncertainty

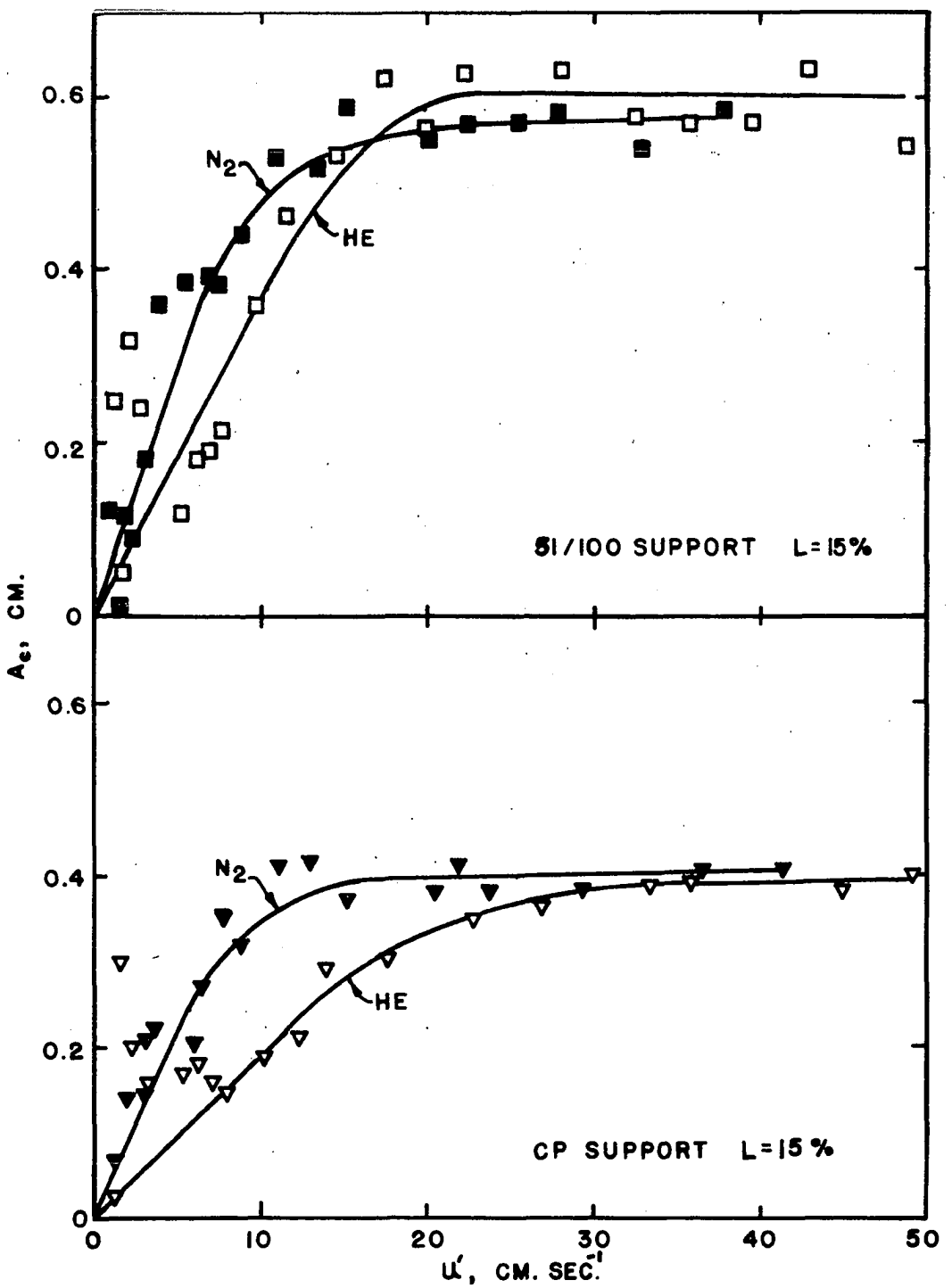

Figure 5. Illustration of coupled eddy diffusion term vs. interparticle gas velocity

of fitting a curve to the data the values of C_c' are subject to rather large errors in some cases. Considering the errors involved, this experimental data seems to confirm that $C_c' \propto D_g'^{-1}$.

Workers who have used the intercept of the H vs. $1/u'$ plots to determine the value of A have tended to discount the coupled A theory because these plots have resulted in straight lines with no noticable positive sloping curve as predicted by this theory. Figure 6 shows $A_c + \frac{B_c'}{u'}$ vs. $\frac{1}{u'}$, using some extremes of $2\lambda d_p$ and C_c' values found in this work and $B_c' = 0.6$. The resulting plots are only very slightly curved due to the fact that the decrease in A_c as $u' \rightarrow 0$ is offset by the rapid increase in B_c'/u'. Both of the sets of hypothetical data yielded distinct intercepts approximately equal to the value of $2\lambda d_p$ chosen. This plot makes it quite clear that the coupling theory of eddy diffusion cannot be substantiated or refuted using the ordinary graphical techniques.

The results in Table 4 indicate that $2\lambda_1 d_p$ and $2\lambda_2 d_p$, the values of A_c as $u' \rightarrow 0$, are approximately equal to the A values evaluated as the $u' = 0$ intercept of the H vs. $1/u'$ plot (see Theory and Calculations). This observation is in agreement with hypothetical data presented in Figure 6 and the discussion presented above. The values of $2\lambda_1 d_p \simeq 2\lambda_2 d_p$ for each support and liquid load (see Table 4) as theory predicts and the differences can be attributed to errors in the C values used in their evaluation.

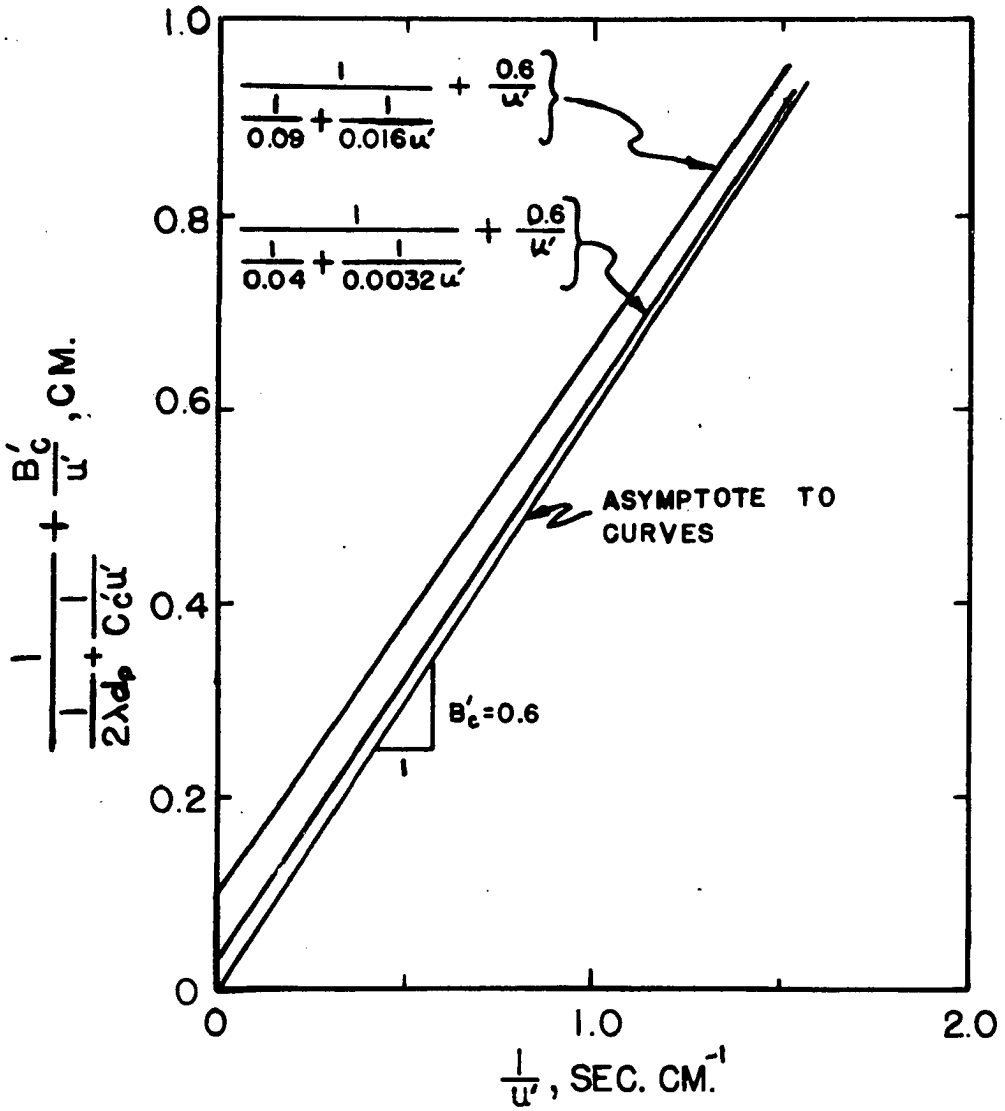

Figure 6. Effect of coupled eddy diffusion term on intercept of plate height vs. reciprocal interparticle velocity plots

Figure 7 shows the fit of typical experimental H vs. u' data to the curve calculated using A_c. This may be compared to Figure 4. The fit is much better at low velocities but somewhat poorer at intermediate velocities.

Longitudinal Diffusion

The longitudinal diffusion term of the van Deemter equation, B', can be estimated from the experimental data with considerable accuracy by measuring the slope of the H vs. 1/u' plot. With the confirmation of the existence of a coupled eddy diffusion term A_c, B' must be considered as the slope of the asymptote (B_c') to the H vs. 1/u' curve rather than the slope of the best straight line through the points (see Figure 6). In all cases, $B_c' > B'$ (see Tables 3 and 4).

The reliability of B_c' can be best tested by noting $B_c'_1/B_c'_2 = D_g'_1/D_g'_2$ and comparing the ratio of B_c' terms found from the experimental data to the ratio of measured or empirically estimated D_g' values. Because the diffusivity of 2-octanone in helium and nitrogen has not been reported in the literature, the Gilliland equation (34) was used to estimate these diffusivities in $cm.^2\ sec.^{-1}$ Considering the errors involved in such empirical estimations of D_g', the theoretical ratio of $D_g'_1/D_g'_2 = 0.255/0.0834 = 3.05$ is probably good to only $\pm$ 0.3 or $\pm$ 10%.

The ratio of $B_c'_1/B_c'_2$ is given in Table 5.

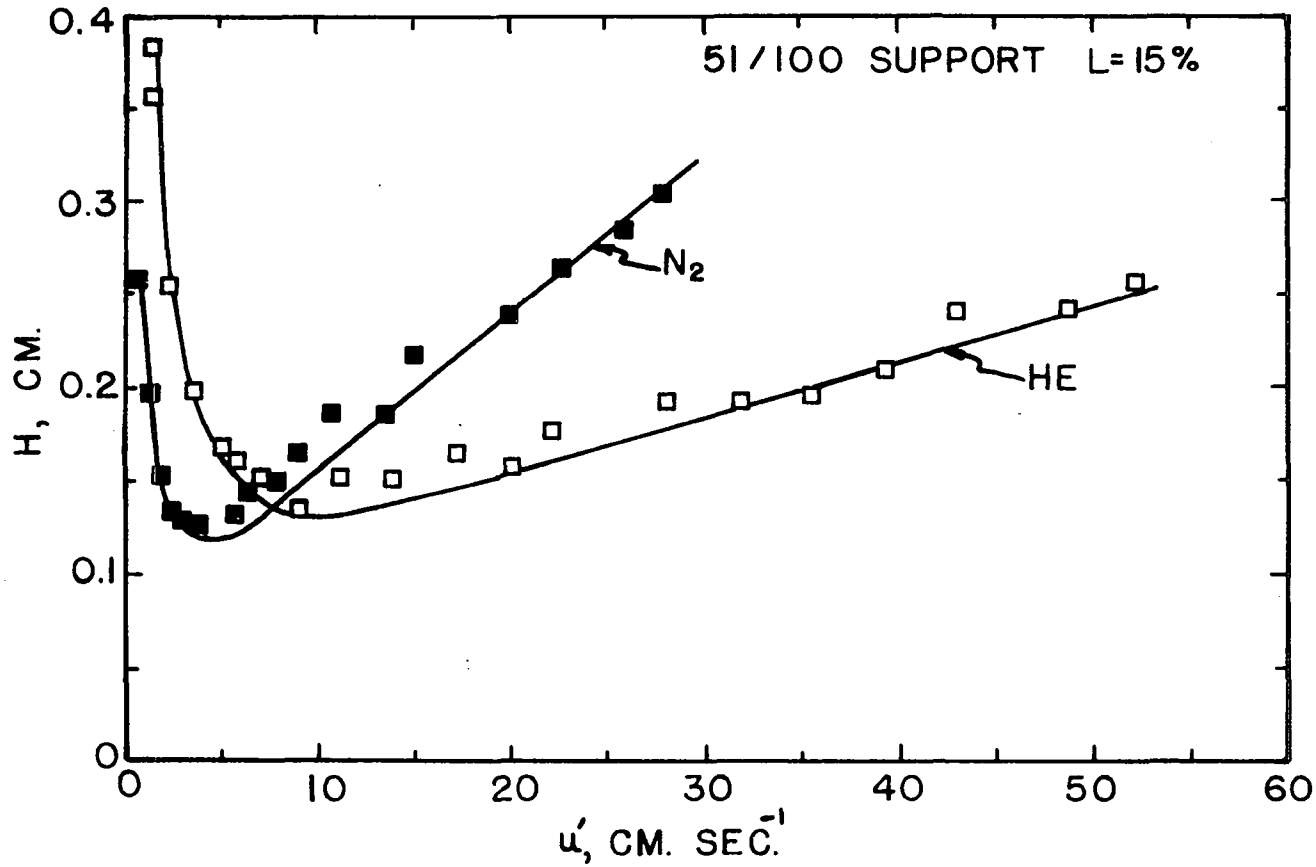

Figure 7. Illustration of fit of experimental data to curve calculated with modified van Deemter equation containing coupled eddy diffusion term

Table 5. Ratio of experimental values of B_c' for 2-octanone eluted with helium and nitrogen

Solid support	Liquid load, L[a]		
	25	15	5
40/100	2.69[b]	2.89	3.00
51/100	2.85	2.95	2.96
55/100	3.00	2.94	3.00
CP	2.83	2.76	2.74

[a]The %w liquid phase on an equal volume of CP.

[b]$B_c'_1/B_c'_2$.

All the experimental ratios are in excellent agreement among themselves regardless of the solid support or amount of liquid phase. All the experimental ratios are less than the theoretical ratio but fall within the estimated error.

The results in Table 4 clearly indicate reductions in B_c' with increases in liquid load and support particle density. A slight influence of liquid load on B was recently noted in the work of De Ford et al. (15). However, Kieselbach (46), Bohemen and Purnell (5, 6) and Perrett and Purnell (58) have reported values of B which are essentially independent of liquid load. The change of B_c' with liquid load found for CP in this work is about the same as found by De Ford et al. However, for the lyophilized supports B_c' showed definite changes with liquid load and particle density. These changes are certainly

significant especially in view of the reliability of the B_c' estimates demonstrated in Table 5.

The longitudinal diffusion term appears in the modified van Deemter equation as $2\gamma D_g'$. The labyrinth constant, γ, has been an empirical correction which has been found to have a magnitude $\simeq 1$ (5, 6, 58). To account for changes in B_c', γ must be influenced by both liquid load and solid support.

Ficks law gives the rate of mass transfer by a diffusional process as:

$$\frac{\partial c}{\partial t} = D\frac{\partial^2 c}{\partial x^2} \qquad (26)$$

where D = diffusivity, cm.^{2} sec.$^{-1}$

c = concentration of solute, g. moles cm.$^{-3}$

t = time, sec.

x = length in direction of diffusion, cm.

The above equation applies to diffusion across a unit cross-sectional area. Since the plate height depends on the standard deviation of the concentration of the solute band in the eluting gas, the plate height then depends on the total amount of solute transported. Therefore, in a chromatographic column, the amount of band spreading resulting from longitudinal diffusion will be proportional to the area available for diffusion.

Two possible diffusional paths are available for a solute molecule, one through the interparticle void, V_v, and the other through the intraparticle void, V_p. The V_v was relatively constant (see Table 6) as measured by the inter-

particle void fraction, ϵ. The V_p varied with solid support particle density and was reduced when liquid phase was added since the liquid occupied a definite volume within the particle. Therefore, γ can be visualized as being the sum of the contributions from the inter- and intraparticle diffusional areas such that:

$$\gamma = \gamma_v + \gamma_p = n_v V_v + n_p V_p \qquad (27)$$

where γ_v = interparticle contribution to γ

γ_p = intraparticle contribution to γ

$n_v V_v$ = interparticle area fraction available for diffusion

$n_p V_p$ = intraparticle area fraction available for diffusion

Because denser particles and increased liquid loads resulted in reduced V_p and γ, the experimental data agrees with this equation.

The exact effect that changes in liquid load and support characteristics have on the constant n_p, which correlates V_p with interparticle area fraction, is unpredictable. The addition of liquid phase might only constrict larger pores while sealing smaller diffusional pathways. Baker et al. (2) measured the rate of diffusion through CP particles impregnated with varying amounts of silicone oil liquid phase. They found that the diffusion rate decreased rapidly (to about $\frac{1}{4}$ the bare packing value) as the amount of liquid was increased to 10% w. Additional increases of liquid phase to 30% w resulted in a slower decrease in the diffusion rate (to about 1/10 the

bare packing value). Above 30% w liquid load the diffusion rate was very small and decreased very little with increasing liquid load. Over the three ranges of liquid loads examined by Baker et al., the plot of changes in diffusion rate with changes in liquid load could be approximated by three straight lines of different slopes. This indicates that n_p in eq. 27 will be nearly constant if the liquid load does not change over too wide a range and γ_p will change linearly with changes in liquid load.

Table 6 shows the effect of solid support density and liquid load on V_p and V_v. The calculated V_p using eq. 23 showed substantial decreases in going from the 40/100 to the 55/100 support with CP lying between these extremes. The V_p can be estimated from the retention volume of air by $V_a - V_v = V_p$. The data in Table 6 indicates that V_p calculated in this manner was always larger than the V_p calculated using eq. 23. This discrepancy was also noted by Bohemen and Purnell (5) who attributed this difference to unavoidable adsorption of the solute. This difference might also be attributed to non-equilibrium in the diffusion of solute molecules within the support packing causing an increase in retention volume. In all cases, the trend of $V_a - V_v$ and V_p was in the same direction with $V_a - V_v$ being 1.0 to 1.5 $cm.^3$ larger per column.

The values of γ presented in Table 6 are subject to some suspicion considering that nearly all values are > 1 and

Table 6. Inter- and intraparticle void volumes as effected by solid support and liquid load

Solid support	Liquid phase, L[a]	Interparticle void fraction, ϵ	Interparticle volume, V_v, cm.^{3}	Intraparticle volume, V_p, cm.^{3}	Retention volume of air, V_a, cm.^{3}	Intraparticle volume, V_a-V_v, cm.^{3}	γ_1[b]
40/100	25	0.425	14.2	11.5	25.6	11.4	1.21
	15	0.405	13.5	13.0	27.1	13.6	1.47
	5	0.386	12.9	14.5	26.2	13.3	1.77
	0	0.407[c]	13.6	15.2			
51/100	25	0.416	13.9	9.3	25.2	11.3	1.12
	15	0.400	13.4	10.8	25.7	12.3	1.27
	5	0.396	13.3	12.3	27.3	14.0	1.39
	0	0.407[c]	13.6	13.0			
55/100	25	0.422	14.1	7.7	22.0	7.9	0.71
	15	0.418	14.0	9.2	24.1	10.1	0.92
	5	0.410	13.8	10.7	25.7	11.9	1.18
	0	0.407[c]	13.6	11.4			
CP	25	0.403	13.5	10.0	25.4	11.9	1.28
	15	0.403	13.5	11.5	26.1	12.6	1.35
	5	0.396	13.1	13.0	27.3	14.2	1.45
	0	0.407[c]	13.6	13.7			

[a]The % w liquid phase on an equal volume of CP.

[b]Calculated using $D_g'_1 = 0.255$ cm.^{2} sec.$^{-1}$.

[c]Average value of ϵ.

theory predicts (14) that $\gamma \leq 1$. The D'_g value used to calculate γ had a maximum error of 10% and cannot account for all the discrepancy noted. The large values of γ must, therefore, be a result of over estimating the value of B'_c. B'_c, the slope of the asymptote to the H vs. $1/u'$ plot, is strongly influenced by u' whose value has been calculated in a number of ways by different investigators.

All data in this work were interpreted (Bohemen and Purnell (5)) using the interparticle velocity, u', at the column outlet pressure and temperature as the correct velocity for use in the modified van Deemter equation. Many other workers have interpreted their data using a velocity, u'_a, calculated considering the total void volume (V_a) available for flow. In all cases, $V_v < V_a$ so that $u' > u'_a$. Therefore, the values of B'_c found using u' are greater than values of B'_c found using u'_a. If u'_a had been used in this work, a maximum value of $\gamma = 0.83$ and a minimum of 0.46 would result. Although u' can be used in the van Deemter equation to give a good fit of the data, it appears that u' does not give good values of B'_c which are in agreement with the theoretical concept of B'_c. Regardless of the value of u used to calculate B'_c, the trends found in this work were the same. Therefore, the correlation in changes of γ with changes in V_p are significant.

The data in Table 6 indicate that γ_1 for the CP support changed less with liquid load than it did for the lyophilized

supports. This may have resulted from a difference in the geometric arrangement in the interparticle void. For example, CP has been shown, using an electron microscope, to consist of relatively large interconnected voids (Dal Nogare and Chiu (11)) while the pores of the lyophilized supports may be interconnected with primarily small pores ($<0.05\mu$). This difference in interconnecting pore size between the two supports would mean the available interparticle diffusional area for the lyophilized support would decrease most rapidly with liquid phase addition resulting in their larger changes in δ. Or alternatively, there might be a difference in the ratio of "dead end" to "through" pores in CP and the lyophilized supports.

In Figure 8, the increase in δ, with increasing V_p is illustrated. When V_p (eq. 23) was used (dashed lines on graph), all three experimental values of δ for one support fell on a straight line, these lines for different supports had different slopes; some with intercepts <0. If $V_p = V_a - V_v$ was used (solid line on graph), all the points fell approximately on one straight line. This may indicate that the retention volume of air gives a truer picture of the intraparticle void diffusional area than does the intraparticle void calculated from density considerations. Examination of eq. 27 shows δ to be a linear function of V_p with slope n_p if $n_v V_v$ is constant. The interparticle void fraction, ϵ, is nearly constant (see Table 6) making it reason-

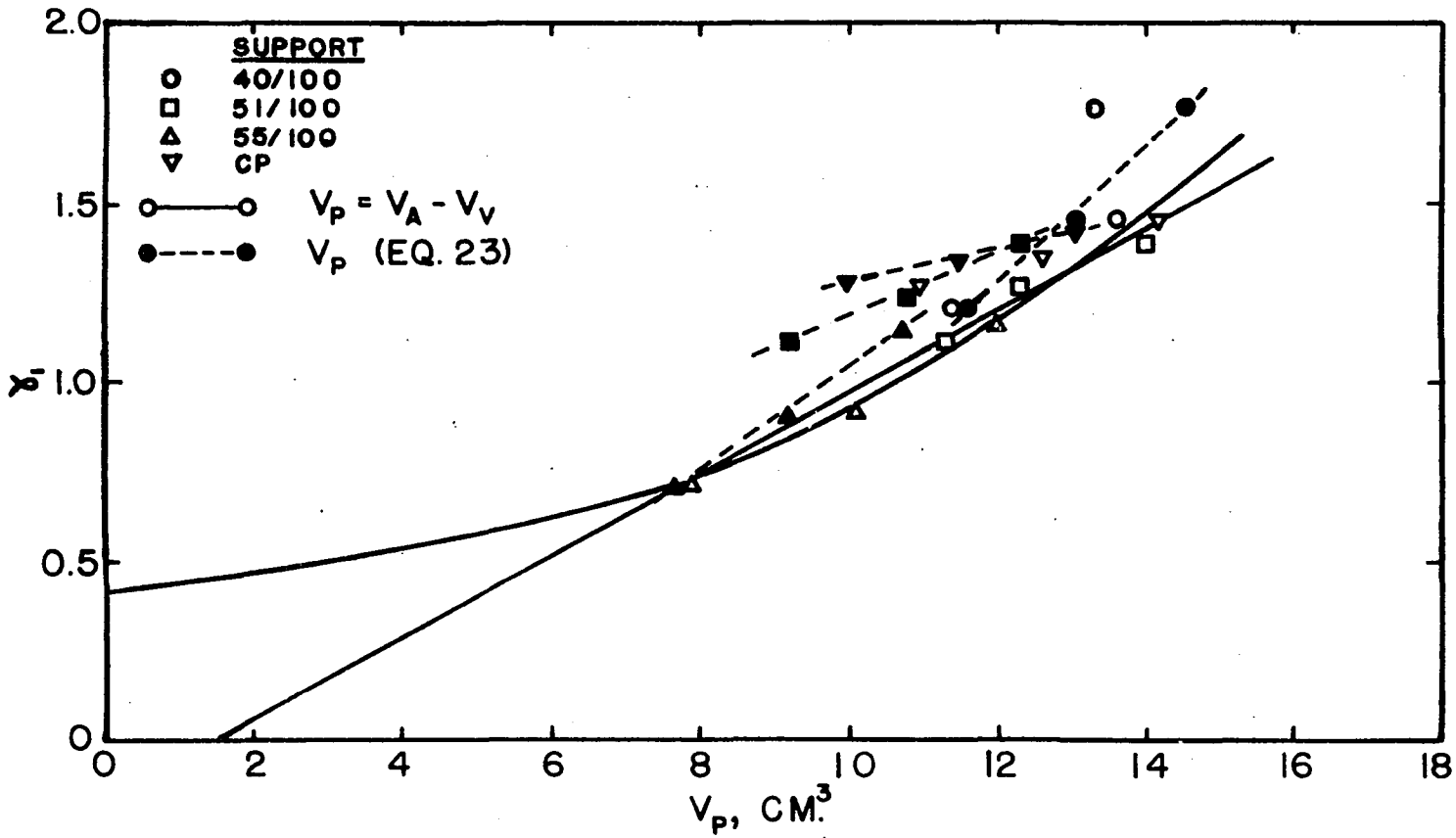

Figure 8. The labyrinth constant vs. intraparticle volume

able to assume $n_v V_v$ constant. Because the straight line intercept of Figure 7 is slightly < 0, it appears that the slope, n_p, is not constant but decreases with liquid load so that γ_v is > 0. The apparent need for n_p to decrease with liquid load is in agreement with the previously cited intraparticle diffusion rate data of Baker *et al.* (2) which indicated that n_p should be only linear over a short range of liquid loads and should be > 0 at high liquid loads. The minimum value of γ at $V_p = 0$ is highly speculative considering the unknown relationship between n_p and L, but appears to be $\simeq 0.4$.

Gas Phase Resistance to Mass Transfer

The importance of including a gas phase non-equilibrium term in the modified van Deemter equation was demonstrated again in this work. The tabulated values of C_g' in Table 3 often exceed C_l. The C_g' terms for the 51/100, 55/100 and CP supports at a given liquid load agreed closely, almost within experimental error which was estimated at $\pm$ 0.0003 sec. The values of C_g', for these columns, showed nearly uniform increases with each increase in L from 5 to 15 and 15 to 25 with perhaps slightly larger increases as L increased from 15 to 25.

The C_g' terms for the 40/100 support were considerably different from the three other supports used. At L = 25, C_g' for the 40/100 support was about 1/3 the C_g' for the other

supports. The pore size distribution data (Figures 3a and 3b) showed the 40/100 support to have the largest number of pores >1 μ. This data might indicate that the open microstructure of the 40/100 solid support allowed more rapid diffusion of the solute molecules into and out of the pores where it contacts the liquid phase. However, if this is so the 51/100 support, which has a more open microstructure than the 55/100 and CP supports, should give smaller C_g' values at a given liquid load than the corresponding values for the 55/100 and CP supports. A small trend in this direction can be detected in the data of Table 3.

The C_g' increased with decreases in L on the 40/100 support which is contrary to the trend seen on the other three supports. A similar reversal with the most porous packing was found in the preliminary studies. The probable explanation is that the 40/100 support, being quite porous, had little mechanical strength and was easily broken during the packing of the columns. When the liquid phase was added to the support, coating and filling the pores, the strength of the packing increased and less break-up resulted during column packing. Break-up of the 40/100 support was indicated by much higher pressure drops across these columns. The formation of fines in the column packing at low liquid loads, may tend to increase flow inhomogenities within the column. This is partially substantiated by the high $2\lambda d_p$ values of the 40/100 support (Table 4). Flow inhomogenities have been shown by

Giddings (28) to make a major contribution to the magnitude of C_g'.

Bohemen and Purnell (7) have shown that columns made with supports having a wide range of particle sizes are less efficient than columns made with supports having a narrow particle size range. They attributed this loss of efficiency to an increase in C term of the original van Deemter equation which did not distinguish C_g' and C_l. The formation of fines, with the 40/100 support would result in a wider range of particle sizes producing a situation similar to the one experimentally treated by Bohemen and Purnell.

The C_g' coefficient has been defined by:

$$C_g' = \omega \frac{d_p^2}{D_g'} \tag{28}$$

where ω is a contribution to C_g' which changes with liquid load and solid support characteristics. Giddings (28), using theoretical considerations has derived an equation for C_g' resulting from flow inhomogenities which included a parameter ω_{fi}. Perrett and Purnell (58) showed $\omega > \omega_{fi}$ and postulated that:

$$C_g' = (\omega_{fi} + \omega_{si}) \frac{d_p^2}{D_g'} = \omega \frac{d_p^2}{D_g'} \tag{29}$$

where ω_{si} is the contribution to C_g' resulting from liquid phase maldistribution. These authors gave:

$$\omega_{fi} = 0.4 - \frac{0.12}{1+k} \tag{30}$$

which has the constants changed slightly from the theoretically derived expression given by Giddings (28). These changes in

constants gave the best fit to their experimental data and that of others.

Table 7 lists the values of k, ω, ω_{fi} and $\omega_{si} = \omega - \omega_{fi}$ found in this study. The values of k did not change enough under the conditions used to make any significant changes in ω_{fi}. There was some indication that eq. 30 yields values of ω_{fi} which are too large as indicated by $\omega_{fi} > \omega$ in two cases.

Table 7. Gas phase resistance to mass transfer data for the elution of 2-octanone by helium

Solid support	Liquid load, L[a]	k	ω[b]	ω_{fi}[c]	ω_{si}[d]
40/100	25	48.9	0.378	0.398	-0.020
	15	27.6	0.723	0.397	0.426
	5	9.5	1.04	0.391	0.649
51/100	25	49.6	0.953	0.398	0.555
	15	29.2	0.665	0.397	0.268
	5	9.1	0.434	0.390	0.044
55/100	25	57.0	1.16	0.398	0.762
	15	31.1	0.723	0.397	0.326
	5	9.7	0.520	0.391	0.129
CP	25	49.3	1.21	0.398	0.812
	15	26.7	0.810	0.397	0.413
	5	9.1	0.347	0.390	-0.043

[a]The % w liquid phase on an equal volume of CP.

[b]$\omega = \dfrac{C_g' D_g'}{d_p^2} = \dfrac{C_g'(0.255)}{(0.0297)^2}$

[c]Calculated using eq. 30.

[d]$\omega_{si} = \omega - \omega_{fi}$.

Assuming the values of ω_{fi} are reasonable estimates, ω_{si} shows a rapid increase with L on the 51/100, 55/100 and CP supports, similar to the findings of Perrett and Purnell (58). These authors felt that the increase in ω_{si} was associated with the filling of anisotropic particle to particle structure giving lateral liquid inhomogenities at high liquid loads. The filling of the interparticle pores seems questionable when Baker et al. (2) have shown that the smallest pores in a support were filled preferentially and the intraparticle pores are primarily $<3\mu$. and the interparticle pores $>20\mu$. Table 6 shows that approximately half the intraparticle void is unfilled at L = 25, making it unlikely that much liquid phase would be free to fill the interparticle pores. It would, therefore, appear that ω_{si} arises from the reduced ability of solute molecules to diffuse in and out of the pores at high liquid loads.

Since $B_c' = 2\gamma D_g'$, $C_g' = \frac{\omega d_p^2}{D_g'}$ and $C_c' = \frac{(\beta d_p)^2}{2 D_g'}$, all are functions of D_g'. In the case of B_c', D_g' was corrected for the intraparticle area available for diffusion by γ. One would also expect intraparticle diffusion to play an important role in C_g' and C_c' so that corrections similar to γ would have to be applied. In general, it was found that increasing particle density and liquid load decreased B_c' and increased C_g' and C_c' as would be expected from the effect of these variables on intraparticle diffusion. However, the corrections for D_g' in these three constants are not parallel

because intra- and interparticle diffusion do not contribute to these terms in equal proportions.

Liquid Phase Resistance to Mass Transfer

The theoretical work of Giddings (24, 27, 29) has pointed to the influence of the pore size and configuration on C_l. The work of Baker et al. (2), in confirmation of the theory of Giddings, showed most of the liquid filling the smaller pores in the packing (capillary liquid) with only a small portion of the total liquid (adsorbed liquid) in a thin layer on the support surface.

The values of C_l tabulated in Table 3 show increases with increasing liquid load as would be expected considering the theory. These data also indicate that C_l for CP was, at every liquid load investigated, less than the corresponding values for the lyophilized supports. In comparing the pore size distributions (Figures 3a and 3b) of CP and lyophilized supports, the lack of fine pores ($<0.1\ \mu$) in CP was an obvious difference. Some of these fine pores in the lyophilized support are pictured as being rather long, compared to their diameter, forming a labyrinth interconnecting the larger pores. In contrast, microphotographs of CP would indicate a structure containing evenly sized pores with a depth approximately equalling their diameter. These fine pores in the lyophilized supports will be filled preferentially making rather deep pools of liquid within the support. These deep pools of

liquid would increase the lag in equilibrium within the stationary phase resulting from the increased penetration of solute molecules and would account for the larger C_1 values for lyophilized supports. These observations were in agreement with the theoretical derivations of Giddings (29) showing $C_1 \propto d^2 D_1^{-1}$, where d is the pore depth and D_1 the diffusivity of the solute in the liquid phase.

Calculations for the lyophilized supports showed the liquid phase volume at L = 25 to be nearly equal to the volume of pores $<0.5\mu$ in diameter. Assuming these supports have similar pore structures for pores $<0.5\mu$ and that the small pores were preferentially filled, it appears reasonable the C_1 should be approximately equal for all supports at equal liquid load as shown in the data. High liquid loads would tend to emphasize any dissimilarities in the pore structure and could account for the high C_1 found for the 55/100 support at L = 25.

Due to the absence of small pores in CP, at L = 25 nearly all pores $<1.0\mu$ will be filled. Even though the diameter of the liquid pools on the support surface of CP will be larger than those on the lyophilized supports, their shallow nature will result in a lower C_1.

Pore size distribution data gives the volume of pores with a specified diameter, but gives no clue as to the depth of the pores. Considering the important role that pore depth

plays in the magnitude of C_l, methods for its evaluation will be needed before correlations between the structural characteristics and C_l can be made.

CONCLUSIONS

A solid support resembling the commercial detergent, Tide, can be made by lyophilizing a mixture of sodium hexamataphosphate (Calgon), sodium sulfate and sodium silicate in about the proportions found in Tide. The porosity and pore size distribution of the lyophilized supports can be readily changed by varying the concentration of the salts in the lyophilized solution; the lower concentrations will result in a support with greater porosity and larger pores (3 - 5μ). As the concentration of salts in the lyophilized solution increased, the very fine pores ($< 0.035\mu$) account for more of the total pore volume.

Changes in support porosity can be easily determined by measuring the support packed density (g. support/cm.^{3} packed volume) if the interparticle void fraction remains constant. This can be accomplished by using a standardized packing technique. It was shown that the particle density (g. support/cm.^{3} particle volume) could have been estimated from the readily measured packed density with reasonable accuracy.

Preliminary data showed the plate height, H, decreased with decreasing solid support density; the 50/100 support produced the minimum H with a slight increase in H when the most porous 42/100 support was used. As the support packed density increased, the rate of change in H with changes in interparticle velocity, u', increased. Increases in H with increased liquid loads at a constant u' was also demonstrated. The

increases in H for the 42/100 compared to the 50/100 support were at least partially caused by break-up of the fragile 42/100 cupport during column packing. The presence of fines within the column packing would tend to increase the resistance to mass transfer in the gas phase and increase H.

A least squares regression of the preliminary data to evaluate the coefficients of the modified van Deemter equation was unsuccessful. The u' and $\bar{u}$ velocities were too similar making the separate contributions of C_g' and C_l non-significant. An increased number of experimental measurements and measurements of H at high u', where u' becomes considerably greater than $\bar{u}$, would prove helpful in obtaining significant coefficients.

The calculation methods of Purnell and co-workers proved satisfactory in the evaluation of the modified van Deemter equation coefficients and were used for the comprehensive studies on three lyophilized supports (40/100, 51/100 and 55/100) and CP each at liquid loads, L, equalling 5, 15, and 25. It was shown that values of C_g' and C_l independent of A and B', could be calculated using these methods if the diffusivity of the solute in the gas, D_g', was known and the values of H at high u' were used.

The coupled eddy diffusion theory of Giddings (26) was confirmed in these comprehensive studies. A method was proposed for calculating A_c at various values of u' using values of B_c', C_g' and C_l evaluated independently of one another.

The determination of A_c was subject to some error because it was evaluated from a difference between the experimental values of H and the contributions of B_c', C_g' and C_l to H. Therefore, values of C_c', calculated as the slope of the A_c vs. u' curves as $u' \rightarrow 0$ were subject to the errors of A_c. Even though the errors in C_c' were substantial, it was shown that its magnitude was proportional to $D_g'^{-1}$ as theory predicts.

The value of $2\lambda d_p$ was shown to be independent of the eluting gas in agreement with theory. Values of $2\lambda d_p$ found using the coupled theory of eddy diffusion were nearly equal to the values found as the intercept of the H vs. $1/u'$ plot. It was shown that this should be an expected result because a plot of $A_c + \frac{B_c'}{u'}$ vs. u' showed an intercept $\simeq 2\lambda d_p$.

The confirmation of the coupled eddy diffusion theory requires that the longitudinal diffusion coefficient, B_c', be evaluated as the slope of the asymptote, through the origin, of the H vs. $1/u'$ plot. Values of $B_c' > B'$ will result in all cases. Although there is some error in estimating the location of the asymptote, the B_c' values determined in this manner showed a great deal of internal consistency because the ratio of B_c' terms for the two eluting gases was nearly constant for all columns and approximately equal to the theoretical ratio. In all cases, B_c' decreased with increased particle density and liquid load. The data indicate that this observation results from a reduction in the intra-

particle diffusional area which appears to be a linear function of V_p, measured by $V_a - V_v$, over a limited range of liquid loads. However, above L = 25, the intraparticle diffusional area appears to be quite small and changed little with further increases in liquid load. The data also indicate that the labyrinth constant, γ, can be written as the sum of inter- and intraparticle contributions, $\gamma_v + \gamma_p$, where $\gamma_p \rightarrow 0$ for non-porous supports or as the liquid phase fills all the available intraparticle spaces. It was speculated, using an uncertain extrapolation of the data, that minimum γ, or γ_v, at $V_p = 0$ is $\simeq 0.4$.

The theoretical contributions of flow inhomogenities within the packing resulting from unequal flow channels can not account for rapid increase in C_g' found with increases in liquid load. It appears that the reduced ability of solute molecules to diffuse in and out of the pores constricted by high liquid loads accounts for these rapid increases in C_g'. This hypothesis is supported by the fact that supports with a dense microstructure containing small pores has larger C_g' contributions than did the more porous packings.

The experimental increases in C_g' and C_c' ($\propto D_g'^{-1}$) and the decrease in B_c' ($\propto D_g'$) with increased liquid load and particle density point to the important contribution that intraparticle diffusion makes in determining the magnitude of these coefficients. The effects of liquid load and particle density do not change these coefficients equally because

intra- and interparticle diffusion contribute in different proportions to each coefficient. Packings with a very open microstructure and yet mechanically strong should give lower C_g' and C_c' and larger B_c' contributions. Large values of B_c' are not extremely serious, however, because their contributions to H at the moderate flow velocities used for analysis would be small.

CP which has been shown to have uniform pores of approximately equal depth and width gave the smallest C_1 values. Theory predicts C_1 will be proportional to the square of the pore depth. The lyophilized support has more fine pores and may give larger C_1 values because the pores are longer and less ramified. To quantitatively substantiate this theory, some direct measure of the pore depth will have to be devised.

The ideal gas chromatographic solid support appears to be one consisting of a very open microstructure allowing rapid passage of the solute molecules in and out of the support. The surface of the large pores should be covered with short pores of uniform small diameter which will hold large quantities of stationary phase. It will be necessary for this support to be mechanically strong so that break-up, resulting in fines, will not occur during column packing.

SUMMARY

A gas chromatographic solid support was made by lyophilizing a mixture of sodium hexametaphosphate, sodium sulfate and sodium silicate. The porosity and pore size distribution of this support could be readily changed by varying the total concentration of salts in the lyophilized solution. This system proved useful in studying the effects of porosity and pore size on plate heights.

Three different lyophilized supports and Chromosorb P (CP) were evaluated at three liquid loads using 2-octanone as the solute and helium and nitrogen as eluting gases. The amount of liquid phase (Carbowax 20M) per packed volume of support was standardized at values equivalent to 5, 15, and 25% w on the CP support. The plate height (H) was measured at a range of interparticle velocities (u') and the data were used to evaluate the constants of the modified van Deemter equation:

$$H = A_c + B_c'/u' + C_g'u' + C_l\bar{u}$$

where $$A_c = \frac{1}{1/2\lambda d_p + 1/C_c'u'}$$

The constants $2\lambda d_p$ and C_c' are the coupled eddy diffusion coefficients proposed by Giddings, B_c' is the coefficient of band spreading by longitudinal diffusion, C_g' is the coefficient for resistance to mass transfer in the gas phase, and C_l is the coefficient for resistance to mass transfer in the liquid phase and $\bar{u}$ the average column interparticle gas velocity.

A new method was devised to calculate A_c at various values of u' and these studies substantiated the coupled eddy diffu-

sion term proposed by Giddings. The maximum values of A_c were nearly equal for all lyophilized supports as theory predicts.

Values of B_c' decreased and C_g' and C_c' increased as support density and liquid load increased. These factors produce reductions in intraparticle volume, and these trends point to the important role played by the intraparticle diffusional area in establishing the magnitude of these constants. The exact effect of changes in intraparticle diffusional area differ for each coefficient because intra- and interparticle diffusion contribute differently to each term.

The pore diameter and length effected C_g' and C_l markedly. Values of C_g' were reduced when the support had a very porous and open microstructure which allowed rapid passage of solute molecules in and out of the support. Deep pools of liquid resulted from filling the long pores in the lyophilized supports and made C_l greater than the corresponding values for CP. The ideal support is therefore visualized as having a very open microstructure which contains short pores of uniform diameter to hold the liquid phase.

BIBLIOGRAPHY

1. Ayers, B. O., Loyd, R. J. and De Ford, D. D. Principles of high speed gas chromatography with packed columns. Analytical Chemistry 33:987-991. 1961.

2. Baker, W. J., Lee, E. H. and Wall, R. F. Chromatographic solid support studies. In Noebels, H. J., Wall, R. F., and Brenner, N., eds. Gas chromatography. pp. 21-32. New York, New York, Academic Press, Inc. 1961.

3. Bens, E. M. Adsorption characteristics of some gas-liquid chromatographic supports. Analytical Chemistry 33:178-182. 1961.

4. Bethea, R. M. and Adams, F. S., Jr. Gas chromatography of the C_1 to C_4 nitroparaffins. Isothermal vs. linear temperature programming. Analytical Chemistry 33:832-839. 1961.

5. Bohemen, J. and Purnell, J. H. Diffusional band spreading in gas chromatographic columns. I. The elution of unsorbed gases. Journal of the Chemical Society 360-367. 1961.

6. Bohemen, J. and Purnell, J. H. Diffusional band spreading in gas-chromatographic columns. II. The elution of sorbed vapors. Journal of the Chemical Society 2630-2638. 1961.

7. Bohemen, J. and Purnell, J. H. Some applications of theory in the attainment of high column efficiencies in gas-liquid chromatography. In Desty, D. H., ed. Gas chromatography, 1958. pp. 6-17. New York, New York, Academic Press, Inc. 1958.

8. Brennan, D. and Kemball, C. Resolution in gas-liquid chromatography. Journal of the Institute of Petroleum 44:14-17. 1958.

9. Carberry, J. J. and Bretton, R. H. Axial dispersion of mass in flow through fixed beds. A. I. Ch. E. Journal 4:367-375. 1958.

10. Cartan, F. O. and Curtis, G. J. Apparatus for the determination of particle density of porous solids. Analytical Chemistry 35:423-424. 1963.

11. Dal Nogare, S. and Chiu, J. A study of the performance of packed gas chromatography columns. Analytical Chemistry 34:890-896. 1962.

12. Dal Nogare, S. and Juvet, R. S., Jr. Gas-liquid chromatography. pp. 132-133. New York, New York, Interscience Publishers. 1962.

13. Decora, A. W. and Dineen, G. U. Gas-liquid chromatography of pyridines using a new solid support. Analytical Chemistry 32:164-169. 1960.

14. Deemter, J. J. van, Zuiderweg, F. J. and Klinkenberg, A. Longitudinal diffusion and resistance to mass transfer as causes of nonideality in chromatography. Chemical Engineering Science 5:271-289. 1956.

15. De Ford, D. D., Loyd, R. J. and Ayers, B. O. Studies on the efficiencies of packed gas chromatographic columns. Analytical Chemistry 35:426-429. 1963.

16. Desty, D. H., Godfrey, F. M. and Harbourn, C. L. A. Operating data on two stationary phase supports. In Desty, D. H., ed. Gas chromatography, 1958. pp. 200-211. New York, New York, Academic Press, Inc. 1958.

17. Desty, D. H. and Goldup, A. Coated capillary columns; An investigation of operating conditions. In Scott, R. P. W., ed. Gas chromatography, 1960. pp. 162-178. London, England, Butterworth and Co., Ltd. 1960.

18. Desty, D. H., Goldup, A. and Whyman, B. H. F. The potentialities of coated capillary columns for gas chromatography in the petroleum industry. Journal of the Institute of Petroleum 45:287-298. 1959.

19. Desty, D. H. and Harbourn, C. L. A. Evaluation of a commercial alkyl aryl sulfonate detergent as a column packing for gas chromatography. Analytical Chemistry 31:1965-1970. 1959.

20. De Wet, W. J. and Pretorius, V. Some factors influencing the efficiency of gas-liquid partition chromatography columns. Analytical Chemistry 30:325-329. 1958.

21. Dimbat, Martin, Shell Development Co., Emeryville, California. [Solid supports and gas chromatographic efficiency.] Private communication. [1958]. Original not available; cited in Keulemens, A. I. M. Gas chromatography. p. 156. New York, New York, Reinhold Publishing Corp. 1959.

22. Ettre, L. S. The effect of the surface area on the separation in gas-liquid partition chromatography. Journal of Chromatography 4:166-169. 1960.

23. Frederick, C. H., Meranda, B. T. and Cooke, W. D. The effect of liquid loading on the efficiency of gas chromatography columns. In Brenner, N., Callen, J. E. and Weiss, M. D., eds. Gas chromatography, pp. 27-36. New York, New York, Academic Press, Inc. 1962.

24. Giddings, J. C. Advances in the theory of plate height in gas chromatography. Analytical Chemistry 35:439-449. 1963.

25. Giddings, J. C. Coiled columns and resolution in gas chromatography. Journal of Chromatography. 3:520-523. 1960.

26. Giddings, J. C. 'Eddy' diffusion in chromatography. Nature 184:357-358. 1959.

27. Giddings, J. C. Liquid distribution on gas chromatographic support; relationship to plate height. Analytical Chemistry 34:458-465. 1963.

28. Giddings, J. C. Nature of gas phase mass transfer in gas chromatography. Analytical Chemistry 34:1186-1192. 1961.

29. Giddings, J. C. Plate height contributions in gas chromatography. Analytical Chemistry 33:962-963. 1961.

30. Giddings, J. C. Plate height of nonuniform chromatographic columns; gas compression effects, coupled columns, and analogous systems. Analytical Chemistry 35: 353-356. 1963.

31. Giddings, J. C. The role of lateral diffusion at a rate controlling mechanism in chromatography. Journal of Chromatography 5:46-60. 1961

32. Giddings, J. C. and Robison, R. A. Failure of the eddy diffusion concept of gas chromatography. Analytical Chemistry 32:867-870. 1960.

33. Giddings, J. C., Seager, S. L., Stucki, L. R. and Stewart, G. A. Plate height in gas chromatography. Analytical Chemistry 32:867-870. 1960.

34. Gilliland, E. R. Diffusion coefficients in gaseous systems. Industrial and Engineering Chemistry 26:681-685. 1934.

35. Glueckauf, E. [Discussion on eddy diffusion] In Desty, D. H., ed. Vapour phase chromatography, 1957. pp. 29-30. New York, New York, Academic Press, Inc. 1957.

36. Glueckauf, E. Theory of chromatography. IX. The 'theoretical plate' concept in column separations. Transactions of the Faraday Society 51:34-44. 1955.

37. Golay, M. J. E. Theory of chromatography in open and coated tubular columns with round and rectangular cross-sections. In Desty, D. H., ed. Gas chromatography, 1958. pp. 36-55. New York, New York, Academic Press, Inc. 1958.

38. Harper, J. M. An apparatus for measuring bulk density of dried milk. Food Technology 16:144. 1962.

39. Hishta, C., Messerly, J. P. and Reschke, R. F. Gas chromatography of high boiling compounds on low temperature columns. Analytical Chemistry 32:1730-1738. 1960.

40. James, A. R. and Martin, A. J. P. Gas-liquid partition chromatography: The separation and micro-estimation of volatile fatty acids from formic acid to dodecanoic acid. The Biochemical Journal 50:679-690. 1952.

41. Jones, W. L. Modifications to the van Deemter equation for the height equivalent to a theoretical plate in gas chromatography. Analytical Chemistry 33:829-832. 1961.

42. Keller, R. A., Bate, R., Costa, B. and Forman, P. Changes occuring with the immobile liquid phase in gas-liquid chromatography. Journal of Chromatography 8: 157-177. 1962.

43. Keulemans, A. I. M. and Kwantes, A. Factors determining column efficiency in gas-liquid partition chromatography. In Desty, D. H., ed. Vapour phase chromatography, 1957. pp. 15-29. New York, New York, Academic Press, Inc. 1957.

44. Khan, M. A. Non-equilibrium theory of gas-liquid chromatography. Nature 186:800-801. 1960.

45. Kieselbach, R. Gas chromatography; source of the velocity independent A term in the van Deemter equation. Analytical Chemistry 33:806-807. 1961.

46. Kieselbach, R. Gas chromatography; the effect of gaseous diffusion on mass transfer in packed columns. Analytical Chemistry 33:23-28. 1961.

47. Kieselbach, R. Theory of plate height in gas chromatography. Analytical Chemistry 32:880-881. 1960.

48. Klinkenberg, A. and Sjenitzer, F. 'Eddy' diffusion in chromatography. Nature 187:1023. 1960.

49. Klinkenberg, A. and Sjenitzer, F. Holding-time distributions of the Gaussian type. Chemical Engineering Science 5:258-270. 1956.

50. Kramers, H. and Alberda, G. Frequency response analysis of continuous flow systems. Chemical Engineering Science 2:173-181. 1953.

51. Landault, C. and Guiochon, G. Etude de l'utilisation du Tiflon comme support en chromatographic gaz-liquide. Application a la separation de corps tris polaires. Journal of Chromatography 9:133-146. 1962.

52. Littlewood, A. B. An examination of column efficiency in gas-liquid chromatography, using columns of wetted glass beads. In Desty, D. H., ed. Gas chromatography, 1958. pp. 23-33. New York, New York, Academic Press, Inc. 1958.

53. Loyd, R. J., Ayers, B. O. and Karasek, F. W. Optimization of resolution-time ratio with packed chromatographic columns. Analytical Chemistry 32:698-701. 1963.

54. Lukes, V., Komers, R. and Herout, V. Ground unglazed tile; a new support for gas-liquid chromatography. Journal of Chromatography 3:303-307. 1960.

55. Martin, A. J. P. and Synge, R. L. M. A new form of chromatogram. The Biochemical Journal 35:1358-1368. 1963.

56. Norem, S. D. Behavior of inert gas packets in chromatographic columns. Analytical Chemistry 34:40-42. 1962.

57. Ottenstein, D. M. Column support materials for use in gas chromatography. Journal of Gas Chromatography 1, No. 4 :11-24. April 1963.

58. Perrett, R. H. and Purnell, J. H. Contribution of diffusion and mass transfer processes to efficiency of gas liquid chromatography columns. Analytical Chemistry 35: 430-439. 1963.

59. Perrett, R. H. and Purnell, J. H. Evaluation of liquid phase mass transfer coefficients in gas chromatography. Analytical Chemistry 34:1336. 1962.

60. Purnell, J. H. The development of highly efficient gas-liquid chromatographic columns. Annals of the New York Academy of Sciences 72:592-605. 1959.

61. Rijnders, G. W. A. [Discussion on gas chromatographic efficiencies] In Desty, D. H., ed. Gas chromatography, 1958. p. 18. New York, New York, Academic Press, Inc. 1958.

62. Sawyer, D. T. and Barr, J. K. Evaluation of support materials for use in gas chromatography. Analytical Chemistry 34:1518-1520. 1962.

63. Sawyer, D. T. and Barr, J. K. Theory and practice of low-loaded columns in gas chromatography. Analytical Chemistry 34:1052-1057. 1962.

64. Scott, R. P. W. and Hazeldean, G. S. F. Some factors affecting column efficiency and resolution of nylon capillary columns. In Scott, R. P. M., ed. Gas chromatography, 1960. pp.144-158. London, England, Butterworth Co., Ltd. 1960.

ACKNOWLEDGEMENTS

The author wishes to express his appreciation to Dr. E. G. Hammond who suggested the research problem and gave guidance and counsel during its progress. Dr. Hammond's help and suggestions during the preparation of the thesis were also appreciated.

The author also wishes to acknowledge the cooperation of Dr. V. H. Nielsen making it possible to complete his graduate training while teaching in the Department of Dairy and Food Industry.

The author is indebted to the Iowa Agricultural Experiment Station for supporting the research and the National Science Foundation for support during the summers of 1962 and 1963.